Food and Chemical Toxicology 133 (2019) 110262

Contents lists available at ScienceDirect

Food and Chemical Toxicology

journal homepage: www.elsevier.com/locate/foodchemtox

Hepatic transcriptional dose-response analysis of male and female Fischer rats exposed to hexabromocyclododecane

Reza Farmahin[a], Anne Marie Gannon[b], Rémi Gagné[a], Andrea Rowan-Carroll[a], Byron Kuo[a], Andrew Williams[a], Ivan Curran[b], Carole L. Yauk[a,*]

[a] Environmental Health Science and Research Bureau, Healthy Environments and Consumer Safety Branch, Health Canada, Ottawa, ON, K1A 0K9, Canada
[b] Regulatory Toxicology Research Division, Health Products and Food Branch, Health Canada, Ottawa, ON, K1A 0K9, Canada

ARTICLE INFO

Keywords:
RNA-Sequencing
Transcriptomics
Toxicogenomics
Mode of action
Benchmark dose (BMD)
Point of departure
Risk assessment

ABSTRACT

Hexabromocyclododecane (HBCD) is a brominated flame retardant found in the environment and human tissues. The toxicological effects of HBCD exposure are not clearly understood. We employed whole-genome RNA-sequencing on liver samples from male and female Fischer rats exposed to 0, 250, 1250, and 5000 mg technical mixture of HBCD/kg diet for 28 days to gain further insight into HBCD toxicity. HBCD altered 428 and 250 gene transcripts in males and females, respectively, which were involved in metabolism of xenobiotics, oxidative stress, immune response, metabolism of glucose and lipids, circadian regulation, cell cycle, fibrotic activity, and hormonal balance. Signature analysis supported that HBCD operates through the constitutive androstane and pregnane X receptors. The median transcriptomic benchmark dose (BMD) for the lowest statistically significant pathway was within 1.5-fold of the BMD for increased liver weight, while the BMD for the lowest pathway with at least three modeled genes (minimum 5% of pathway) was similar to the lowest apical endpoint BMD. The results show how transcriptional analyses can inform mechanisms underlying chemical toxicity and the doses at which potentially adverse effects occur. This experiment is part of a larger study exploring the use of toxicogenomics and high-throughput screening for human health risk assessment.

1. Introduction

Hexabromocyclododecane (HBCD) is a brominated flame retardant (BFR) that is used in polystyrene foams for thermal insulation in buildings, upholstery textiles, and electrical equipment housings (Alaee et al., 2003). HBCD is persistent throughout the environment and has strong potential for both long-range environmental transport and bioaccumulation/biomagnification (Wania and Dugani, 2003; Law et al., 2006). HBCD was listed for global elimination under Annex A (Elimination) of the Stockholm Convention on Persistent Organic Pollutants (POPs) (UNEP, 2013a; UNEP, 2013b). However, because of its biopersistence, HBCD is still leaching from existing products and high levels are still found in the human diet (Barghi et al., 2016), house dust (Fromme et al., 2014; Lignell et al., 2015), human tissues, breast milk, and blood (Lignell et al., 2015; Fromme et al., 2016). Thus, further studies are required to better assess and understand the potential health hazards from exposure to HBCD.

HBCD primarily affects liver function, eliciting a variety of adaptive and adverse responses following exposure. For example, oral exposure increases liver weight in a dose-dependent manner in both male and female rats (van der Ven et al., 2006; Chengelis, 1997, 2001; Zeller and Kirsch, 1969, 1970; Gannon et al., Submitted). While the mechanism involved in liver weight increase is not fully understood, it is thought that liver enlargement may be a hepatic physiological adaptation to increased xenobiotic metabolism activity following HBCD exposure (Chengelis, 2001; Maronpot et al., 2010). Liver proteome analysis of female rats administered 3 and 30 mg HBCD/kg bw/day (mkd) for 7 days showed significant changes in abundance of 13 proteins involved in metabolic processes (gluconeogenesis/glycolysis, amino acid metabolism, lipid metabolism) and oxidative stress response (Miller et al., 2016a). Several studies support that HBCD increases reactive oxygen species (ROS) generation and liver oxidative stress in different animals (Miller et al., 2016a; Feng et al., 2013; Zhang et al., 2008a). A previous study using a reporter gene assay in a transfected hematoma cell line suggested that HBCD is an agonist of the pregnane X receptor (PXR) (Fery et al., 2009). In addition, gene expression analysis of rat livers from a subacute 28-day repeat-dose oral toxicity study (30 or 100 mkd of HBCD) showed up-regulation of genes involved in phase I and II metabolism pathways, while genes involved in peroxisome proliferator-activated receptor (PPAR)-mediated regulation of lipid metabolism,

* Corresponding author. Environmental Health Science and Research Bureau, 50 Colombine Drive, Tunney's Pasture, Ottawa, ON, K1A 0K9, Canada.
E-mail address: carole.yauk@canada.ca (C.L. Yauk).

https://doi.org/10.1016/j.fct.2018.12.032
Received 19 October 2018; Received in revised form 13 December 2018; Accepted 20 December 2018
Available online 27 December 2018

triacylglycerol metabolism, and cholesterol biosynthesis were down-regulated (Canton et al., 2008). Thus, HBCD exposure affects a broad range of physiological processes in the liver.

The adaptive and adverse effects of HBCD exposure are not limited to liver function and have been reported for a number of different biological processes in various organisms. For example, it is well established that HBCD interferes with the immune system (Cato et al., 2014; Hinkson and Whalen, 2009, 2010; Almughamsi and Whalen, 2016; Hachisuka et al., 2010). Moreover, previous studies have indicated some potential for neurotoxic (Reistad et al., 2006), neurodevelopmental (Roze et al., 2009), and developmental effects (Hong et al., 2015) of HBCD. HBCD also acts as an endocrine disruptor in rats, with significant effects on the thyroid hormone axis that include increased thyroid weight, increased thyroid stimulating hormone (TSH) and decreased circulating T4 levels, as well as decreased thyroid follicle size (Chengelis, 2001; Ema et al., 2008; van der Ven et al., 2006, 2009; Saegusa et al., 2009; Berger et al., 2014; Gannon et al., Submitted). *In vitro* studies have also shown that HBCD is an antagonist of androgen and progesterone receptors (Hamers et al., 2006). While a broad spectrum of biological effects is induced by HBCD, the molecular mechanisms underlying these adaptive/adverse effects are not fully understood.

To explore the mechanisms underlying HBCD-induced hepatotoxic effects, we applied whole-genome RNA-sequencing (RNA-seq) to liver samples from male and female Fischer rats exposed to a technical mixture of HBCD administered orally via feed for 28 days. We also investigated whether gene expression changes and pathway perturbations associated with other target organ toxicities are evident in the liver transcriptome. These findings were compared with HBCD-induced apical endpoints to determine whether alterations in gene expression could be linked to various previously described physiological and pathological outcomes. Finally, we used benchmark dose (BMD) analysis to explore the doses at which transcriptional effects occur. The overarching goal of this study is to advance our understanding of HBCD-induced toxicological effects and the application of gene expression analysis in human health risk assessment.

2. Materials and methods

2.1. Animals and exposures

Detailed animal exposures have been described elsewhere (Gannon et al., Submitted). Briefly, a mixture of 1,2,5,6,9,10-hexabromocyclododecane (CAS number 3194-55-6; technical HBCD; 95% purity) consisting of 11% α-HBCD, 9% β-HBCD, and 79% of γ-HBCD was purchased from Sigma-Aldrich (St. Louis, MO). Powdered AIN93G diet (Reeves, 1997) was purchased from Dyets Inc. (Bethlehem, PA). Technical refers to the commercially available HBCD mixture, which is used in the manufacturing of products. Diets were prepared as previously described (Gannon et al., Submitted). Forty male and 40 female Fischer 344 rats at 34–37 days of age were randomly divided into groups of 10 male and 10 female rats and exposed to either control, low (L), medium (M), or high (H) doses (0, 250, 1250, or 5000 mg HBCD/kg diet, respectively). These dietary concentrations of 250, 1250, and 5000 mg HBCD/kg diet were converted to doses of 18.7, 94.1, and 399.6 mg/kg BW/day for males, and 20.2, 102.0, and 430.0 mg/kg BW/day for females, respectively, based on observed mean weekly food consumption/mean BW (Gannon et al., Submitted) After 28 days, rats were sacrificed by exsanguination via the abdominal aorta under isoflurane anesthesia. At necropsy, the weights of select organs were recorded and gross pathological assessments were conducted. Liver, serum, and adipose were also collected for residue determination. Animal handling and treatment procedures were conducted according to the Guidelines of the Canadian Council of Animal Care and were approved by the Health Canada Animal Care Committee (Ottawa, ON, Canada).

2.2. RNA extraction and cDNA synthesis

RNA was extracted from frozen liver tissue using Direct-zol RNA MiniPrep kits with on column DNA digestion (Zymo Research Corp. Irvine, CA) according to the manufacturer's instructions. RNA was quantified using a NanoDrop spectrophotometer (Thermo Fisher Scientific Inc., Wilmington, DE, USA), and quality confirmed using a 2100 Bioanalyzer (Agilent Technologies, Mississauga, ON, Canada). RNA samples with RNA integrity numbers (RINs) greater than 7.0 were used for RNA-seq experiments.

2.3. RNA-sequencing (RNA-seq)

Preparation of RNA-seq libraries was carried out in randomized batches (8 samples/batch, 10 batches, for a total of 80 samples). Poly-A RNA enrichment was performed using 1.5 μg of total RNA from each sample and DynaBeads® mRNA DIRECT Micro kits (Life Technologies, Canada). Fragmentation and cDNA library preparation was carried out using RNase III and Ion Total RNA-seq kits v2 (Life Technologies, Canada). Fragmented libraries were ligated with 3' barcode adapters from the Ion Xpress™ RNA-seq Barcode 1–96 Automated Library Construction Kit (Life Technologies, Canada). Each sample received its own unique barcode (1–80). Libraries were then PCR amplified using the Platinum® PCR SuperMix, High Fidelity (Life Technologies, Canada), and quantified using an Agilent® Tape Station High Sensitivity DNA Screentape. Each sample was diluted/equalized to 250 pM. All 80 libraries were then pooled together to a final concentration of 50 pM. The Ion Chef™ instrument, Ion P1™ chips (version 3), and Ion PI™ HI-Q Chef Kits (Life Technologies, Canada) were used for emulsion PCR, enrichment, and chip loading. All chips were sequenced using the Ion Proton™ sequencer and the Ion Proton™ HI-Q™ Sequencing Kit (Life Technologies, Canada).

2.4. RNA-seq data analysis

The complete data sets are publicly available through the Sequence Read Archive (SRA) at http://www.ncbi.nlm.nih.gov/sra, project number PRJNA395549. The Proton™ Torrent Server version 4.4.2 interpreted the sequencing data and generated uBAM files for each barcoded sample. Reads were trimmed to remove low quality read prefixes and suffixes with cutAdapt (https://cutadapt.readthedocs.org/en/stable/). Trimmed reads were aligned to the reference genome (Rnor5.0 release 80) using STAR (Dobin et al., 2013) and Bowtie (Langmead and Salzberg, 2012). Gene counting was performed with HT-Seq count (http://www.huber.embl.de/users/anders/HTSeq/doc/count.html); the m parameter was set to "intersection-nonempty" using the Ensembl GTF annotation (Rnor5.0v80). Data quality was assessed by generating NOISeq plots (Tarazona et al., 2015). "Present" transcripts were defined as having $\geq$ 1 CPM in 50% of the biological replicates for at least 1 exposure group. Present genes were processed by the EdgeR package (McCarthy et al., 2012) for analysis of differentially expressed genes (DEGs) in the RNA-seq data. Normalization was performed using TMM (Robinson and Oshlack, 2010) and DEGs were identified using the GLM model. Genes with false discovery rate (FDR) $\leq$0.05 and absolute fold change (FC) $\geq$1.5 were identified as DEGs. DEG lists, FC, and FDR were obtained by using the TopTags function with the default parameters in the EdgeR package.

Hierarchical cluster analysis was conducted using all DEGs (from any group) using the mean of log CPM for replicates of each control or treatment groups. The distance metric was set to 1-(Spearman correlation).

2.5. Mode of action (MOA) analysis

To explore MOA in HBCD-exposed rat livers, previously published transcriptomic data from rat livers for chemicals with well-defined

MOAs were obtained from the Gene Expression Omnibus (GEO) (Gong et al., 2014), in addition to published gene lists that can be used to predict rat hepatocarcinogenicity and genotoxicity (Gusenleitner et al., 2014). Gong et al. (2014) produced RNA-seq expression profiles from the livers of male Sprague-Dawley rats treated with 15 chemicals (three rats per chemical) or matched vehicle controls using Illumina RNA-Seq technology. The 15 chemicals spanned five MOAs in total, with three chemicals per MOA: three receptor-mediated molecular initiating events (PPARα, constitutive androstane receptor (CAR)/PXR, and aryl hydrocarbon receptor (AHR) agonism); and two non-receptor-mediated MOAs (DNA damage and cytotoxicity). Normalized read counts from the Magic pipeline (Thierry-Mieg and Thierry-Mieg, 2006) were used for the analysis. The Magic normalized RNA-Seq index of expression is comparable to a normalized microarray logarithmic luminosity. The log ratios were obtained for each sample by subtracting the mean of the route of exposure (intraperitoneal injection or oral gavage) and vehicle type (nutritive or non-nutritive) matched controls. Genes with multiple NCBI Gene IDs were averaged and the data were filtered using only genes that had a p-value less than 0.05 from an ANOVA with at least one observation with a FC > 1.5 relative to controls. A nearest shrunken centroid (NSC) analysis (Tibshirani et al., 2002) was then conducted using the filtered data set for each MOA independently. The standardized centroid is the mean expression level for each gene in a class divided by its within-class standard deviation. The standard centroid for each class is then shrunken toward the overall centroid to produce the nearest shrunken centroid. The method employs a shrinkage parameter that is used to control the number of features used to construct the classifier. This analysis was conducted using the pamr library (T. Hastie et al., 2014) in the R statistical environment (R Core Team, 2015).

Using the results from the NSC analyses, gene set enrichment analyses (GSEA) were conducted for each of the five MOAs in the R statistical environment (R Core Team, 2015). GSEA was conducted using the Fisher's Exact Test on the DEGs identified from the EdgeR analysis for males and females (independently).

We also used a published gene list derived from a study that identified gene set classifiers to predict genotoxicity and carcinogenicity in rat livers (Gusenleitner et al., 2014). The authors used 1221 liver gene-expression profiles obtained from rats treated with 127 chemicals to develop the classifiers. A GSEA was conducted on the rat liver expression profiles from our study to determine if the classifier gene sets for genotoxicity or carcinogenicity were enriched in our HBCD data sets.

2.6. BMD modeling

Approach #1. Gene counts (for transcripts denoted as “present” as defined above) were transformed and normalized using the variance-stabilizing transformation function of the DeSeq2 package (Love et al., 2014) for BMD modeling. Normalized data sets were grouped according to BMDExpress (Yang et al., 2007) requirements and imported into BMDExpress (version 1.41). DEGs (FDR p ≤ 0.05 and FC ≥ |1.5|) in at least one dose were statistically fit to all available models (Hill, Power, Linear, and Polynomial 2°) and a best-fit model was selected. Best-fit models were selected based on the following criteria: (1) a nested chi-square test cutoff of 0.05 to choose between linear and polynomial models; followed by (2) the lowest Akaike Information Criterion (AIC) for all of the Hill, Power, Linear and Polynomial models; and (3) a goodness-of-fit p-value > 0.1. Other parameters applied for modeling included: power restricted to ≥1, maximum iterations of 250, confidence interval of 0.95, and benchmark response (BMR) of 1.349 standard deviations (which corresponds to a shift in the mean transcriptomic response of 10% above assumed background)(Yang et al., 2007). The selection of the Hill model was restricted by applying a flag to the model if the *k* parameter was less than 1/3 of the lowest positive dose. If a Hill model was flagged, the next best model with a goodness-of-fit p-value > 0.05 was selected. In the case where no model had a p-value > 0.05, probes that fit Hill models were considered and the lowest BMD value (only BMD derived from Hill models excluding flagged models) was multiplied by 0.5 for use in subsequent analyses. The data sets were mapped to Ingenuity Pathway Analysis (IPA) pathways (downloaded on December 15, 2015) using the Defined Category Analysis feature in BMDExpress.

Approach #2. The US National Toxicology Program (NTP) recently held an expert panel to review their proposed approach for modeling of genomic data (Phillips et al., 2018). This led to a very recent update to BMDExpress to implement the recommendations of the panel (URL: https://www.sciome.com/bmdexpress/). Thus, we re-analyzed the data sets using parameters in accordance with these recommendations (NTP, 2018). Specifically, Williams' Trend tests (Williams, 1971) were applied to statistically filter out genes that did not exhibit a dose-response (p-value < 0.05) and additional filtering removed genes that did not have a FC > 1.5. To derive BMD values for genes, a model (Hill, Power, Linear, Polynomial 2,3, Exponential 2, 3, 4 and 5) that best described the data was selected. The constant variance parameter was unchecked. Model fitting and selection algorithms were identical to those in BMDExpress 1.41. Using the Defined Category Analysis feature in BMDExpress, genes that had a BMD were mapped to pathways from the Ingenuity Pathway Analysis knowledgebase (IPA; downloaded on June 26, 2018). Probes and genes with the following criteria were removed: promiscuous probes, gene BMD > highest dose from category descriptive statistics, curve fit p-value < cutoff (0.0001), genes with BMD/BMDL > 20.0, genes with BMDU/BMD > 20.0, and genes with BMDU/BMDL > 40.0. For probe set to gene conversion, the correlation cutoff for conflicting probe sets was set to 0.5 by default. For analyzing Defined Category Analysis results, only pathways with number of genes ≥ 3 (genes that pass all criteria in the analysis) and percentage of pathway ≥ 5% were selected.

2.7. BMDExpress Data Viewer parameters

BMD Analysis and Defined Category Analysis files were exported from BMDExpress. The exported files were uploaded to BMDExpress Data Viewer (Kuo et al., 2016) for visualization of gene and pathway BMDs using Summary Visualization Tools. Genes that had BMD values greater than the highest dose and BMD/BMDL ratios > 5 were removed [filters based on the US EPA's Benchmark Dose Software (BMDS, version 2.60)] (Davis et al., 2011), which gives a warning message when a BMD/BMDL ratio is greater than five). Frequency distributions of significant genes with BMDs were plotted, and genes within these distributions were identified and used to explore genes and pathways with similar response thresholds. The frequency distribution of gene BMDs for both males and females showed two distinct modes: Mode 1 (genes with BMD values between 1 and 2200 mg HBCD/kg diet) and Mode 2 (genes with BMD values between 2700 and 5000 mg HBCD/kg diet).

2.8. Bioinformatics analysis

Enriched canonical pathways, upstream regulators, and diseases were identified in IPA using all DEGs, as well as those DEGs that could be modeled to derive a BMD in BMDExpress. For the latter, the two modes in the gene BMD distribution plots were analyzed separately. Significant pathways were identified using Fisher's exact tests (unadjusted p ≤ 0.05). Upstream regulators were identified using Z-scores in IPA, which takes into account the direction of change in gene expression in the data sets: a Z score ≥2 was set to identify potentially activated upstream regulators, and a Z score of ≤ −2 was set to identify that the upstream regulator was significantly inhibited. Pathways, upstream regulators, or diseases that did not have at least four significant genes were eliminated from the analysis. In addition, VennPlex was used to identify common and uniquely altered genes between male and female (Cai et al., 2013).

2.9. Genomic-based approaches to predict POD

BMDs within mode 1 were used to produce a median BMD for: (1) the 20 most significantly enriched pathways with the lowest BMDs; (2) the 20 most significant upstream regulators; (3) the 20 DEGs with the largest FCs relative to controls; and (4) the lowest significant pathway BMD (sometimes referred to as 'the most sensitive pathway') as described previously (Farmahin et al., 2016). In addition, we present the three lowest pathway BMDs that had at least three genes and 5% of the pathway affected. From here forward we refer to a BMD derived from an apical endpoint as a BMD_a, and from a transcriptional endpoint as a BMD_t for clarity. Route-adjusted BMD and the 95% lower confidence limit of benchmark dose (BMDL) values for HBCD in mg HBCD/kg diet were converted to mg/kg-day (mkd) based on observed food intake in the rats (Gannon et al., Submitted).

3. Results

HBCD-related effects of exposure to HBCD for 28 days in male and female Fischer rats in our parallel study are fully described in Gannon et al. (Gannon et al., Submitted). The results of the repeated dose oral toxicity study showed effects of HBCD on multiple organs in Fischer male and female rats including the liver, thyroid gland, immune system, and endocrine system. Further, residue analysis conducted on liver, serum, and adipose tissues showed that concentrations of HBCD at all doses in males were significantly lower than those in females, suggesting sex-dependent differences in metabolism of HBCD.

3.1. General toxicogenomic findings

In total, there were 428 and 250 DEGs in males and females, respectively, in at least one treatment group across all doses. The number of DEGs increased with HBCD dose in both sexes, with 68, 107, and 383 DEGs in males, and 10, 75, and 220 DEGs in females, for the 250, 1250, and 5000 mg/kg diet, respectively (Fig. 1; complete lists in Tables S1–S2). Twenty percent, 17%, and 26% of the DEGs in females were in common with male rats for the low-, medium-, and high-dose groups, respectively. Hierarchical cluster analysis of DEGs showed a distinct separation between male and female rats. The male cluster was subdivided into two sub-clusters with all controls in one and all treated samples in the other. The female cluster had two sub-clusters comprising (1) control and low dose, and (2) medium and high dose (Fig. S1).

The most up- and down-regulated DEGs in the highest dose group in males and females (Table 1) are involved in circadian rhythm and lipid metabolism, detoxification of xenobiotics, conjugation of hormones, production of cellular energy, cytoskeletal dynamics, cell growth, pheromone response, and neuronal activity (Table 1).

HBCD altered the expression of several transporter genes involved in carrying different molecules in both sexes. The most notable increases induced by HBCD were for genes involved in xenobiotic and bile acid transport, sugar transport, and mitochondrial anion transporters, while expression levels of neurotransmitter transporters were decreased (Table S3).

There were 58 genes in common between the sexes (Table 2). These genes are involved in a number of important cellular functions including: 1) metabolism of xenobiotics, steroid-, and hormone-related functions (14 genes); 2) glucose and lipid metabolism (seven genes); 3) fibrosis (seven genes); 4) cell cycle growth/arrest (six genes); 5) circadian regulation (four genes); 6) oxidative stress (three genes); 7) DNA replication and degradation (three genes); 8) immune and inflammatory response (two genes); 9) homeostasis of cellular nucleotides (two genes); 10) cation/anion transporter (two genes); and 11) two genes linked to neuronal development (Table 2). Overall, effects on gene expression in both sexes were relatively modest. The largest changes in expression occurred in cytochrome P450 2B1 (*Cyp2b1*; 13.5-

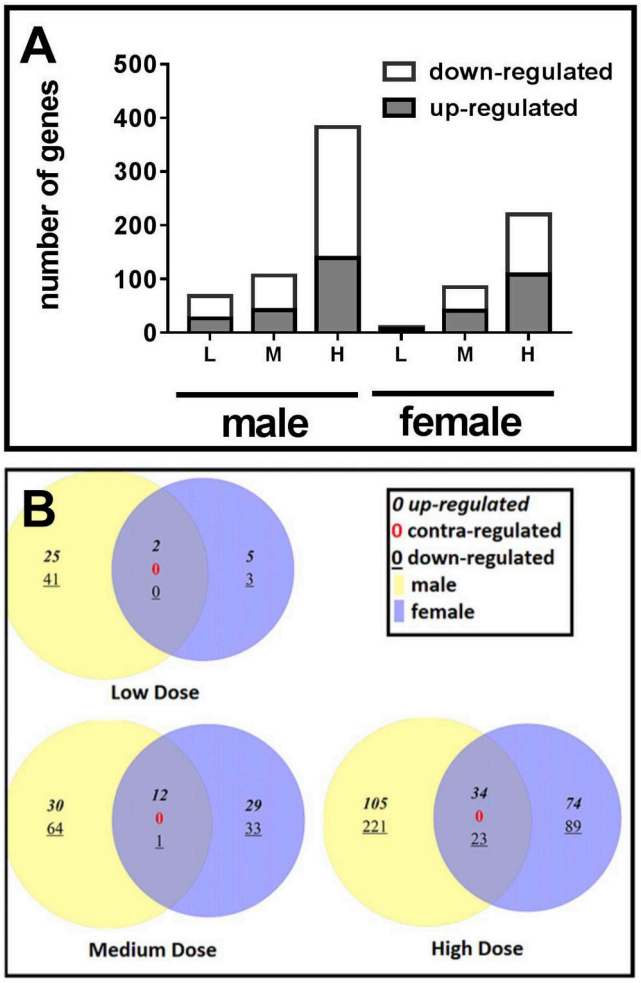

Fig. 1. RNA-seq analysis was carried out on total RNA from livers from male and female Fischer rats exposed to a technical mixture of HBCD for 28 days. A dose-response was apparent for the number of significantly up- and down-regulated genes in males and females (*panel A)*. Up- and down-regulated genes are shown by gray and white colors. Distinct sets of genes were significantly differentially expressed (fold change ≥ 1.5 and FDR *p*-value ≤ 0.05) in the low, medium, and high dose treatment groups (250, 1250, and 5000 mg HBCD/kg diet, respectively) in males versus females (*panel B*). Up-, down-, and contra-regulated genes in males and females are shown by bold italic, under-lined, and red bold, respectively. (For interpretation of the references to color in this figure legend, the reader is referred to the Web version of this article.)

and 14-fold in males and females, respectively), nuclear receptor subfamily 1, group D, member 1 (*Nr1d1;* 8.3- and 9.6-fold in males and females, respectively), and metallothionein (*Mt1;* 4.8- and 4.4-fold in males and females, respectively). Other notable genes in common between the sexes and their key functions are shown in Table 2 and discussed in supplementary materials.

3.2. Nearest shrunken centroid (NSC) analysis

An NSC analysis was used on previously published high-quality RNA-seq data (Gong et al., 2014) to derive a list of genes linked to specific MOAs (Table S4:S8). These gene lists were used for GSEA to determine if the genes were enriched in the HBCD-treated livers. The PXR/CAR gene set was enriched in male and female rats at all doses (Fig. 2; Table S9). Genes in the PXR/CAR gene set are listed in Table S10. The AHR gene set was enriched to a lesser extent for the medium and high doses in female rats only. GSEA did not reveal enrichment for gene sets involved in the other MOAs (i.e., PPARα, DNA damage, or

Table 1
Functions of the most up- and down-regulated DEGs in the highest dose group in males and females.

Functions	Gene Symbol	Gene name	Males					
			L		M		H	
			FDR	FC	FDR	FC	FDR	FC
circadian rhythm and lipid metabolism	*Dbp*	albumin D-box binding protein	0.87	−1.1	0.96	1.1	0	**2.9**
detoxification of xenobiotics	*Ces2e*	carboxylesterase 2E	0.91	1.1	0.07	2.1	0	**2.9**
production of cellular energy	*Mt-nd4*	subunit 4 of mitochondrial NADH dehydrogenase	0.4	2.0	0.87	1.2	0.019	**2.9**
circadian rhythm	*Gnb2l1*	guanine nucleotide binding 2L1	0	**−79.2**	0	**−295.6**	0	**−525.1**
cytoskeletal dynamics	*Acta1*	actin	0	**−51.0**	0	**−28.0**	0	**−174.4**
cell growth	*Sfrp2*	secreted frizzled-related protein 2	0	**−39.0**	0	**−210.1**	0	**−117.5**
Functions	**Gene Symbol**	**Gene name**	**Females**					
			L		M		H	
			FDR	FC	FDR	FC	FDR	FC
pheromone response	*Mup5*	major urinary protein 5	0.98	−1.4	0.87	−1.6	0.01	**14.6**
lipid metabolism	*Scd2*	stearoyl-coenzyme A desaturase 2	0.06	4.3	0	**11.4**	0	**13.3**
hormone and xenobiotic metabolism	*Ste2*	estrogen sulfotransferase enzyme	0.97	−1.8	0.77	−2.0	0.02	**12.8**
neuronal activity	*Slc6a1*	solute carrier 6a1	1	1.0	0.96	−1.1	0.02	**−3.8**
circadian rhythm	*Ccrn4l*	carbon catabolite repression 4 like	0.81	−1.7	0	**−3.6**	0	**−3.8**
neuronal activity	*Apba2*	amyloid beta (A4)	0.98	1.1	0.64	−1.4	0	**−3.6**

Significant and non-significant fold changes are indicated in bold and normal font, respectively.

cytotoxicity; Table S9).

A similar approach was used to derive gene lists that are predictive of genotoxicity and carcinogenicity in rat liver in a previous study (Gusenleitner et al., 2014). GSEA on these gene sets did not predict that HBCD is genotoxic or carcinogenic (data not shown) and is in keeping with the literature.

3.3. BMD_t analysis

BMD_ts could be produced for 175 of 430, and 158 of 253 DEGs in males and females, respectively. $BMD(L)_t$s are shown in Tables S1–S2. Of the modeled genes, 27 (9%) were in common between male and female rats.

Genes identified in BMD modes 1 and 2 in male and female rats. A histogram of the BMD_t distribution revealed a very clear bi-modal distribution in both male and female rats (Fig. 3). In males, 86 genes were in mode 1 (1–2200 mg HBCD/kg diet) and 89 genes were in mode 2 (2700–5000 mg HBCD/kg diet); in females, there were 93 genes in mode 1 and 65 genes in mode 2.

Pathway analysis of BMD_t modes 1 and 2 in male and female rats. The genes within modes 1 and 2 were analyzed separately in IPA to identify perturbed pathways (Table 3). Lipopolysaccharide/interleukin-1 (LPS/IL-1) mediated inhibition of retinoid X receptor (RXR) function and xenobiotic metabolism signaling were enriched in males in both modes 1 and 2, and only in mode 1 in females. Estrogen biosynthesis was also enriched in males in mode 1. In mode 1 of female rats, four additional pathways were enriched: glucocorticoid receptor signaling and nuclear factor (erythroid-derived 2)-like 2 (NRF2)-mediated oxidative stress (cellular stress), PXR/RXR activation, and AHR signaling (Table 3). Notable pathways identified in mode 2 include PPARα/RXRα activation (in males) and hepatic fibrosis/hepatic stellate cell activation (in females).

Upstream regulators identified for BMD_t modes 1 and 2 in male and female rats. The genes within each BMD_t mode were analyzed in IPA to identify significantly activated/inhibited upstream regulators of the perturbed genes (Table 4).

Nine upstream regulators were in an activation state in males in mode 1. Four of these regulators are involved in regulation by nuclear receptors: [PXR (*Nr1i2*), CAR (*Nr1i3*), TO-901317 (CAR agonist), hepatocyte nuclear factor 4 alpha (*Hnf4 a*; *Nr2a1*)]. Two regulators are involved in anti-fibrogenic activity (miR-9-5p and miR-133a-3p). Two regulators (miR-124-3p and miR-423-5p) are involved in suppression and promotion of cell growth and proliferation, respectively. Finally, miR-128-3p is involved in anti-inflammation response (Table 4). In males in mode 2, 18 upstream regulators were identified in an activation state and one was inhibited. These activated regulators are associated with a variety of biological processes including cell proliferation (eight upstream regulators), fibrosis (three regulators), immune response (two regulators), transport of glucose and bile salts [(Solute Carrier Family 13 Member 1(*Slc13a1*)], and response to oxidative stress (miR-200b-3p).

In females in mode 1, expression patterns were consistent with six upstream regulators being activated and four inhibited. Activated upstream regulators in mode 1 of females are involved in AHR and PPARα signaling, glucose and lipid metabolism, liver regeneration, resistance to cell stress, and immune response. Inhibited upstream regulators are involved in promotion of cell proliferation, angiogenesis, steroidogenesis, and progesterone signaling. Seven upstream regulators were enriched in female rats in mode 2 that are involved in suppressing cell proliferation (miR-486-3p and miR-202-3p), anti-fibrotic activity (miR-133a-3p and let-7a-5p), and regulation of endocrine disruption (daidzein) (Table 4).

Disease gene set enrichment in BMD_t modes 1 and 2 in male and female rats. Table 5 shows the enrichment of genes within the HBCD data sets that are associated with diseases and other functional annotations in IPA ($p \leq 0.05$; relevant to liver). Although there was no enrichment of genes associated with any disease in mode 1 for male rats, in mode 2 three diseases were identified: proliferation of liver cells, hepatic steatosis, and fibrosis of liver. In female rats, the following disease gene lists were enriched: liver cancer, cholestasis, and necrosis of liver in mode 1, and inflammation of liver in mode 2 (Table 5).

3.4. Derivation of a transcriptional point of departure (POD)

Approach #1. $BMD(L)_t$ values were used to derive a POD. The transcriptional BMDs ranged from 66 to 104 mg/kg/day in males, and 65–94 mg/kg/day in females. Transcriptional candidate PODs were derived from the mean BMD_t of genes in mode 1 from the following

Table 2
List of common genes affected in male and female rats with BMDt (L) values and in which expression was significantly changed in at least one treatment group (FDR adjusted p value ≤ 0.05, Fold Change (FC) ≥ 1.5).

Function	Gene Symbol	Gene name	Males								Females							
			L		M		H		BMD_t	$BMDL_t$	L		M		H		BMD_t	$BMDL_t$
			FDR	FC	FDR	FC	FDR	FC	(mkd)[‡]	(mkd)[‡]	FDR	FC	FDR	FC	FDR	FC	(mkd)[‡]	(mkd)[‡]
xenobiotic, steroid, and hormone metabolism	*Ugt1a8*	UDP glucuronosyltransferase 1 a8	0.1	1.3	0.0	**1.5**	0.0	**1.7**	11	4	0.9	1.1	0.0	**1.6**	0.0	**1.8**	57	39
	LOC100910877	cytochrome P450 3A1-like	0.2	1.5	0.0	**2.5**	0.0	**3.4**	16	8	0.9	−2.3	0.8	−1.8	0.0	**8.0**	NA	NA
	Ephx1	epoxide hydrolase 1	0.2	1.3	0.0	**1.5**	0.0	**1.6**	20	5	1.0	1.1	0.5	1.3	0.0	**1.5**	407	272
	Sdr42e1	short chain dehydrogenase/reductase 42E	0.8	1.1	0.0	**1.5**	0.0	**2.1**	53	36	1.0	1.1	0.0	**1.8**	0.0	**1.8**	50	36
	Cyp3a2	cytochrome P450 3A2	0.6	1.3	0.0	**2.4**	0.0	**2.3**	54	37	0.9	−2.1	0.8	−1.8	0.0	**7.3**	NA	NA
	Cyp3a23/3a1	cytochrome P450	0.6	1.3	0.0	**2.2**	0.0	**2.8**	54	37	1.0	−1.1	0.7	1.5	0.0	**5.9**	350	243
	Cyp2c13	cytochrome P450 2A13	1.0	−1.0	0.0	**2.7**	0.0	**3.8**	66	43	1.0	−1.7	0.8	−1.6	0.0	**9.4**	NA	NA
	Ces2j	carboxylesterase 2J	0.6	1.3	0.0	**1.7**	0.0	**2.0**	67	44	0.1	**1.5**	0.0	**2.0**	0.0	**2.3**	10	3
	Cyp3a18	cytochrome P450	0.8	1.1	0.2	1.4	0.0	**1.6**	97	56	1.0	1.1	0.2	1.6	0.0	**2.4**	111	63
	Ces2i	carboxylesterase 2i	0.1	1.6	0.0	**1.8**	0.0	**2.0**	NA	NA	1.0	1.2	0.0	**2.2**	0.0	**2.1**	55	38
	Cyp2b2	cytochrome P450 2B2	0.0	**2.8**	0.0	**3.9**	0.0	**3.9**	NA	NA	0.0	**2.0**	0.0	**3.4**	0.0	**3.0**	NA	NA
	Ces2a	carboxylesterase 2a	0.2	1.4	0.0	**1.7**	0.0	**1.7**	NA	NA	0.6	1.3	0.0	**2.0**	0.0	**1.9**	52	37
	Cyp2b1	cytochrome P450 2B1	0.0	**3.8**	0.0	**11.1**	0.0	**13.5**	NA	NA	0.0	**4.5**	0.0	**15.9**	0.0	**13.9**	NA	NA
	Ugt2a1	UDP glucuronosyltransferase 2a1	0.2	1.4	0.0	**2.2**	0.0	**2.3**	NA	NA	0.1	1.5	0.0	**2.2**	0.0	**1.9**	NA	NA
BMD_t mean									***49***	***30***							***137***	***92***
glucose and lipid metabolism	*Aldh1a1*	aldehyde dehydrogenase 1 family	0.9	1.1	0.0	**1.9**	0.0	**2.0**	53	36	1.0	1.1	0.0	**1.7**	0.0	**1.9**	71	46
	Pla2g12a	phospholipase A2	0.8	1.2	0.0	**1.8**	0.0	**2.0**	75	47	1.0	1.0	0.3	1.4	0.0	**1.7**	138	71
	Cpt1a	carnitine palmitoyltransferase I	0.9	1.0	0.3	1.3	0.0	**1.5**	228	171	1.0	−1.2	0.0	**1.8**	0.0	**1.8**	NA	NA
	Adipor2	adiponectin receptor 2	0.8	1.1	0.9	−1.1	0.0	**−1.7**	259	189	1.0	−1.1	0.4	−1.3	0.0	**−1.5**	350	243
	Ppard	peroxisome proliferator-activated receptor delta	1.0	−1.1	0.9	−1.1	0.0	**−1.8**	313	219	1.0	1.0	0.4	−1.3	0.0	**−1.7**	257	191
	Insig1	insulin induced gene 1	1.0	−1.0	0.7	−1.2	0.0	**−1.7**	328	227	0.1	−1.8	0.2	−1.5	0.0	**−1.7**	4	1
	LOC100912565	major urinary protein-like	0.9	1.1	0.8	1.1	0.0	**1.5**	334	231	1.0	−1.6	0.8	−1.8	0.0	**12.2**	NA	NA
BMD_t mean									***227***	***160***							***164***	***110***
fibrosis	*Actg1*	actin	0.7	1.2	0.9	−1.1	0.0	**−1.6**	283	203	0.9	−1.2	0.5	−1.3	0.0	**−1.7**	382	259
	Mfhas1	malignant fibrous histiocytoma as1	0.9	1.1	0.4	−1.5	0.0	**−1.9**	335	231	1.0	1.1	0.9	−1.1	0.0	**−2.0**	268	197
	Tgfb3	transforming growth factor, beta 3	0.8	−1.2	0.5	−1.4	0.0	**−2.0**	394	260	1.0	1.1	0.8	−1.2	0.0	**−1.8**	318	226
	Msn	moesin	0.3	−1.5	0.2	−1.6	0.0	**−1.8**	NA	NA	1.0	1.0	0.5	−1.3	0.0	**−1.7**	317	226
	Hspa4l	Heat Shock Protein A4L	0.9	−1.1	0.5	−1.5	0.0	**−2.1**	NA	NA	1.0	−1.1	0.5	−1.4	0.0	**−1.9**	397	267
	Myh10	myosin, heavy chain 10, non-muscle	0.1	−1.7	0.1	**−1.7**	0.0	**−2.0**	NA	NA	1.0	−1.1	0.4	−1.3	0.0	**−1.6**	365	251
	Ctgf	connective tissue growth factor	0.2	−1.9	0.1	−2.1	0.0	**−2.1**	NA	NA	1.0	−1.2	0.7	−1.2	0.1	**−1.7**	NA	NA
BMD_t mean									***338***	***232***							***341***	***238***
cell cycle growth	*Srms*	Src-Related Kinase Lacking C-Terminal Regulatory Tyrosine And N-Terminal Myristylation Sites	1.0	−1.0	0.5	−1.4	0.0	**−2.1**	340	234	0.8	−1.4	0.4	−1.4	0.0	**−1.9**	NA	NA
	Cdc25b	cell division cycle 25b	0.8	−1.2	0.4	−1.7	0.0	**−2.4**	NA	NA	0.9	−1.5	0.2	−2.2	0.0	**−2.8**	152	74
	Flt1	fms-like tyrosine kinase 1	0.2	−1.8	0.0	**−2.1**	0.0	**−2.5**	NA	NA	1.0	1.1	0.7	−1.3	0.0	**−1.9**	331	233
	Usp2	ubiquitin-specific peptidase 2	0.2	−2.0	0.1	−2.0	0.0	**−2.9**	NA	NA	0.8	−1.5	0.0	**−3.2**	0.0	**−2.8**	55	38
	Efna1	Ephrin A1	0.1	1.5	0.0	**1.6**	0.0	**1.8**	NA	NA	1.0	1.1	0.5	1.2	0.0	**1.5**	397	267
	Gadd45b	growth arrest and DNA-damage-inducible, beta	0.3	1.7	0.0	**2.5**	0.0	**2.2**	NA	NA	0.9	1.3	0.0	**3.0**	0.0	**4.4**	49	35
BMD_t mean									***340***	***234***							***197***	***129***

(*continued on next page*)

Table 2 (*continued*)

Function	Gene Symbol	Gene name	Males								Females							
			L		M		H		BMD_t	$BMDL_t$	L		M		H		BMD_t	$BMDL_t$
			FDR	FC	FDR	FC	FDR	FC	(mkd)‡	(mkd)‡	FDR	FC	FDR	FC	FDR	FC	(mkd)‡	(mkd)‡
circadian regulation	*Nr1d2*	nuclear receptor	1.0	1.0	0.3	1.6	0.0	**2.4**	101	58	1.0	1.1	0.5	1.3	0.0	**2.4**	231	175
	Per3	Period Circadian Clock homolog 3	0.9	−1.2	0.9	1.2	0.0	**3.1**	243	180	0.9	1.5	0.8	1.3	0.0	**2.4**	377	257
	Nr1d1	nuclear receptor	0.0	**2.5**	0.0	**4.0**	0.0	**8.3**	NA	NA	0.6	1.8	0.0	**4.6**	0.0	**9.7**	46	33
	Cry1	cryptochrome circadian clock 1	0.3	−1.3	0.0	**−1.4**	0.0	**−2.4**	NA	NA	1.0	−1.1	0.0	**−1.5**	0.0	**−2.1**	76	49
BMD_t mean									***172***	***119***							***182***	***128***
oxidative stress	*Mt1*	melatonin receptor 1A	0.9	−1.2	0.7	1.5	0.0	**4.4**	291	208	1.0	1.3	0.4	1.9	0.0	**4.4**	273	200
	Gsta3	glutathione S-transferase alpha 3	0.2	2.0	0.0	**2.5**	0.0	**2.9**	NA	NA	1.0	1.0	0.0	**1.8**	0.0	**2.1**	60	41
	Gpx2	glutathione peroxidase 2	0.1	2.1	0.0	**3.1**	0.0	**2.7**	NA	NA	1.0	1.1	0.0	**2.5**	0.0	**2.0**	40	30
BMD_t mean									***291***	***208***							***124***	***90***
DNA replication and degradation	*Pir*	pirin (iron-binding nuclear protein)	0.5	1.3	0.1	**1.5**	0.0	**1.5**	91	53	1.0	1.1	0.1	1.5	0.0	**1.6**	99	58
	Tatdn3	TatD DNase Domain Containing 3	0.8	1.3	0.7	1.3	0.0	**2.0**	373	250	0.8	1.4	0.3	1.4	0.0	**1.7**	NA	NA
	Dnase1l3	Deoxyribonuclease I Like 3	0.3	−1.6	0.1	**−1.9**	0.0	**−2.2**	NA	NA	1.0	1.1	0.8	−1.2	0.0	**−1.9**	332	234
BMD_t mean									***232***	***152***							***216***	***146***
immune and inflammatory response	*Cd4*	Cd4 molecule	0.8	−1.1	0.8	−1.1	0.0	**−1.7**	262	191	1.0	1.1	0.9	−1.1	0.0	**−1.6**	305	219
	Cd5l	CD5 Molecule Like	0.8	−1.1	0.8	−1.1	0.0	**−1.5**	NA	NA	0.8	1.2	0.4	−1.3	0.0	**−1.7**	NA	NA
BMD_t mean									***262***	***191***							***305***	***219***
homeostasis of cellular nucleotides	*Ak4*	adenylate Kinase 4	0.6	−1.3	0.3	−1.5	0.0	**−2.0**	114	22	1.0	−1.2	0.4	−1.4	0.1	**−1.7**	401	269
	Upp2	uridine phosphorylase 2	1.0	−1.1	0.8	1.2	0.0	**2.5**	339	233	1.0	1.2	0.0	**2.3**	0.0	**3.3**	65	44
BMD_t mean									***226***	***128***							***233***	***156***
cation/anion transporter	*Slco1a4*	solute carrier organic anion transporter 1a4	0.6	1.2	0.1	1.5	0.0	**1.9**	64	17	0.5	1.4	0.0	**1.7**	0.0	**2.3**	39	13
	Abcc3	ATP-binding cassette	0.9	1.2	0.4	1.5	0.0	**2.0**	355	241	1.0	1.2	0.0	**2.0**	0.0	**2.1**	79	50
BMD_t mean									***210***	***129***							***59***	***32***
neuronal development	*Lppr1*	plasticity-related gene 3	0.8	−1.2	0.5	−1.5	0.0	**−2.5**	355	242	1.0	−1.0	0.0	**−2.1**	0.0	**−2.8**	76	49
	Cyfip2	cytoplasmic FMR1 interacting protein 2	0.5	−1.5	0.0	**−2.0**	0.0	**−1.9**	96	55	0.9	−1.2	0.1	**−1.6**	0.0	**−2.0**	89	55
synaptic transmission	*Panx2*	Pannexin 2	0.4	1.4	0.3	1.4	0.0	**1.6**	NA	NA	0.9	1.3	0.0	**2.1**	0.0	**2.4**	66	44
BMD_t mean									***226***	***148***							***77***	***49***
endocytic transport	*Ehd3*	EH domain containing 3	0.7	−1.2	0.1	−1.5	0.0	**−1.7**	101	57	0.9	1.2	1.0	−1.0	0.0	**−1.6**	NA	NA
cytoskeletal protein	*Des*	Desmin	0.8	−1.2	0.5	−1.4	0.0	**−1.7**	NA	NA	1.0	−1.1	0.0	**−1.7**	0.5	−1.2	90	54
unclear	*Sh3d21*	SH3 domain containing 21	0.6	1.6	0.6	1.6	0.0	**2.7**	NA	NA	1.0	1.1	0.1	2.0	0.0	**2.0**	100	58
N/A	*AABR07004397.2*	N/A	0.8	1.2	0.0	**1.9**	0.0	**2.6**	53	37	0.9	1.6	0.3	1.9	0.0	**3.8**	308	221
apoptosis-predicted	*Ube2z*	ubiquitin-conjugating enzyme E2Z	0.8	−1.1	0.5	−1.3	0.0	**−1.5**	365	246	1.0	1.1	0.7	−1.2	0.0	**−1.5**	286	208

L (low), M (medium), and H (high) indicates 250, 1250, and 5000 mg/kg hexabromocyclododecane (HBCD)/day in diet, respectively. Significant and non-significant DEGs are shown in bold and normal font, respectively.
‡Route -adjusted BMD_t(L) values in mg/kg HBCD/day in diet were converted to mg/kg-day (mkd) based on observed food intake in the rats (Anne M Gannon, Submitted).

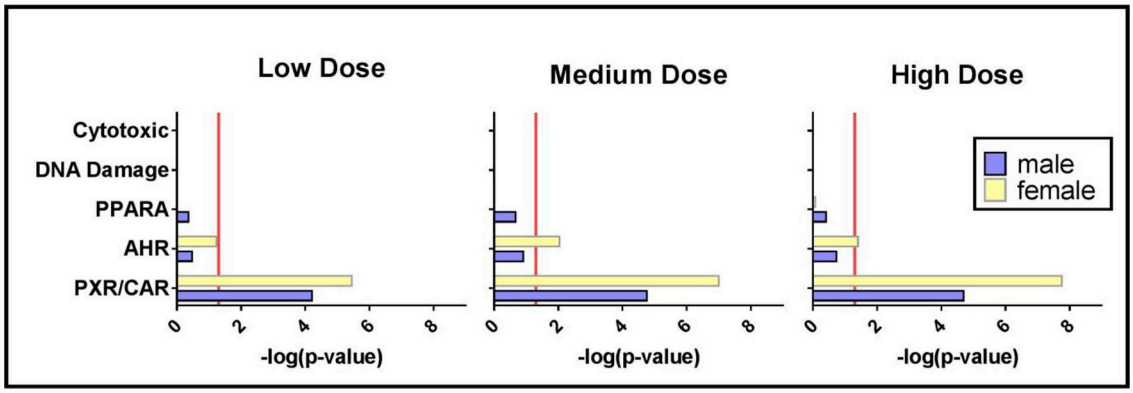

Fig. 2. MOA analysis using pre-defined gene sets from Gong et al. (2014). Gene set enrichment analyses were conducted to determine if the predictive gene sets were enriched in the low, medium, or high dose HBCD treatment groups. The red lines represent a threshold of the −log (*p-value)* of 1.3 (*p* value = 0.05). (For interpretation of the references to color in this figure legend, the reader is referred to the Web version of this article.)

gene lists: (1) the 20 significantly enriched pathways with the lowest BMD_ts (Table 3); (2) the BMD_ts of genes that are regulated by the 20 most statistically significantly enriched ($p \leq 0.05$) upstream regulators with an absolute z-score > 2 (Table 4); (3) the 20 genes with the largest FC relative to controls (Table 6); and (4) the lowest overall pathway BMDt (Table 7). Our previous study showed that these BMD_ts are very good predictors of the doses at which apical effects occur and can be used for POD estimation. We focussed on mode 1 to derive a conservative estimate of the dose at which transcriptional perturbations occur. The median $BMD(L)_t$s for the significant pathways, upstream regulators, largest FC genes, and lowest overall pathway BMD, respectively, are 77(43), 104(46), 84(50), 66(43) mkd (LPS/IL1-mediated inhibition of RXR function) in males, and 73(47), 94(51), 65(44), and 71(46) mkd (LPS/IL1-mediated inhibition of RXR function) in females.

Approach #2. We also employed the NTP's proposed approach to obtain BMD_t values derived for all responsive genes. Following genomic dose-response analysis, genes with BMD were mapped to IPA pathways (downloaded on June 26, 2018). The pathway with the lowest BMD_t value in males was Thyroid Hormone Metabolism II (via Conjugation and/or Degradation) and in females was Acetone Degradation I (to Methylglyoxal). The BMD (BMDL – BMDU) values derived from these pathways were 7.2 (4.3–13) and 3.2 (1.3–7.6) mg/kg bw-day, respectively (Table 7). The second 'most sensitive' pathways in both males and females were Melatonin Degradation I, Nicotine Degradation II and

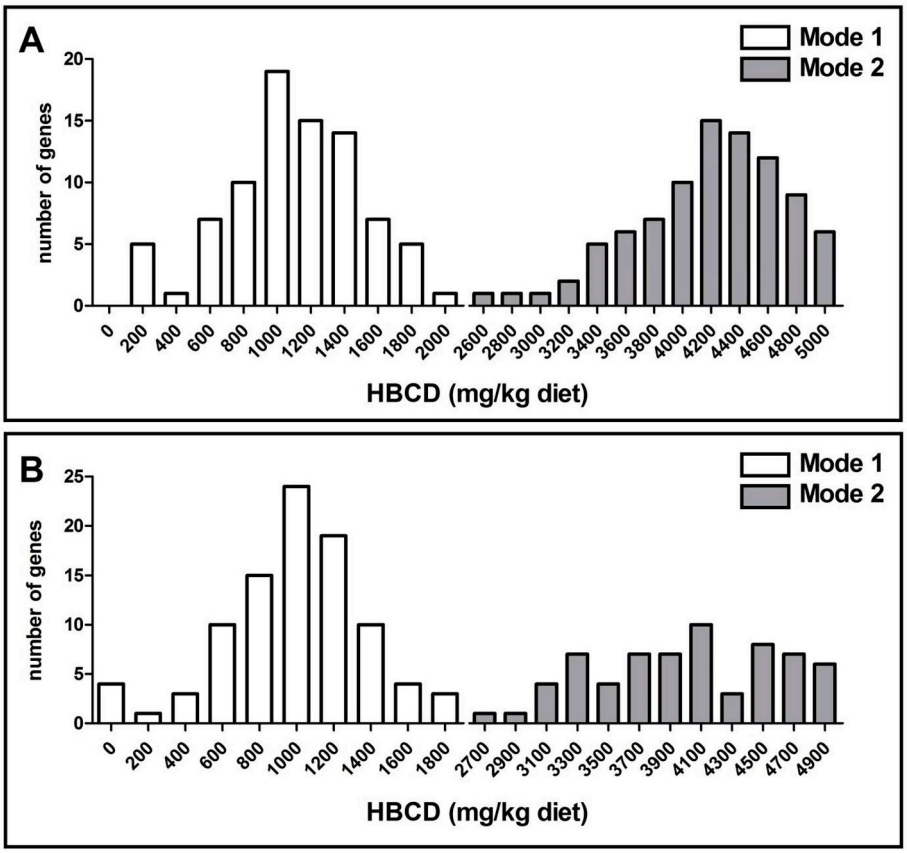

Fig. 3. Distributions of gene BMD_t values in male (*A*) and female (*B*) rats exposed to HBCD for 28 days. Only significant DEGs (FDR $p \leq 0.05$, FC ≥ 1.5) were included.

Table 3
Pathway enrichment of modes 1 and 2 in the gene BMD_t distribution (Fig. 3) in male and female rats following 28 days of exposure to HBCD.

Males

Ingenuity Canonical Pathways	p value	BMD_t (mkd)‡	$BMDL_t$ (mkd)‡	# genes	Molecules
LPS/IL-1 Mediated Inhibition of RXR Function	0.00	67	43	6	*ABCG8,ABCG5,ALDH1A1,Gstm3,CYP3A5,CYP2C19*
Xenobiotic Metabolism Signaling	0.00	78	47	5	*ALDH1A1,Gstm3,CYP3A5,PPP2R1B,CYP2C19*
Estrogen Biosynthesis	0.00	77	37	4	*CYP3A5,CYP2C18,HSD17B2,CYP2C19*
POD estimation		***77***	***43***		
Germ Cell-Sertoli Cell Junction Signaling	0.00	362	245	4	*TGFBR2,TUBA1A,TGFB3,ACTG1*
PPARα/RXRα Activation	0.00	370	233	4	*TGFBR2,GPD2,TGFB3,ADIPOR2*
LPS/IL-1 Mediated Inhibition of RXR Function	0.01	323	225	4	*CPT1A,ABCC3,NDST1,CHST15*
Xenobiotic Metabolism Signaling	0.02	361	244	4	*ABCC3,NDST1,AHR,CHST15*

Females

Ingenuity Canonical Pathways	p value	BMD_t (mkd)‡	$BMDL_t$ (mkd)‡	# genes	Molecules
LPS/IL-1 Mediated Inhibition of RXR Function	0.00	71	46	5	*GSTA3,CYP3A7,ALDH1A1,GSTA1,ABCC3*
Xenobiotic Metabolism Signaling	0.01	71	46	5	*GSTA3,CYP3A7,ALDH1A1,GSTA1,ABCC3*
PXR/RXR Activation	0.00	75	48	4	*CYP3A7,ALDH1A1,GSTA1,ABCC3*
Aryl Hydrocarbon Receptor Signaling	0.00	71	46	4	*GSTA3,MYC,ALDH1A1,GSTA1*
NRF2-mediated Oxidative Stress Response	0.01	84	51	4	*GSTA3,GPX2,GSTA1,DNAJB9*
Glucocorticoid Receptor Signaling	0.03	79	49	4	*SGK1,POU2F2,GTF2E1,TAT*
POD estimation		***73***	***47***		
Hepatic Fibrosis / Hepatic Stellate Cell Activation	0.00	323	229	4	*MYH10,CCR5,Flt1,TGFB3*
Agranulocyte Adhesion and Diapedesis	0.00	341	238	4	*MYH10,CXCL14,ACTG1,MSN*

Median BMD_t and BMD_tL (mg/kg per day) were calculated for significantly enriched pathways in male and female rats. Only pathways with a p-value $\leq$ 0.05 and a minimum of 4 genes were included herein. BMD medians for pathways enriched in mode 1 were for POD prediction. Pathways enriched in modes 1 and 2 are shown by white and gray color, respectively. ‡Route -adjusted $BMD_t(L)$ values in mg/kg HBCD/day in diet were converted to mg/kg-day (mkd) based on observed food intake in the rats (Anne M Gannon, Submitted).

III, and Superpathway of Melatonin Degradation. The pathways with the third lowest BMD_t values were Bupropion Degradation and Acetone Degradation I (to Methylglyoxal) in males, and PXR/RXR Activation in females.

4. Discussion

We used RNA-seq analysis to query the molecular alterations induced by HBCD exposure in male and female rat livers. Functional enrichment analysis revealed that HBCD disrupts the expression of genes associated with a variety of toxicological effects including: (1) increased metabolism of xenobiotic compounds, steroids, and hormones; (2) increased nuclear receptor activity; (3) oxidative stress; (4) alterations in cellular proliferation; (5) disrupted immune and inflammatory responses; (6) perturbed metabolism of glucose and lipids; (7) potential disruption in hormonal balance; (8) fibrosis; and (9) disturbed circadian regulation. Signature analysis suggests that at least some of these effects may be mediated through the CAR/PXR signaling pathway. While we observed distinct gene expression profiles in males and females, the biological functions associated with the altered genes do not significantly differ between sexes. BMD_t modeling revealed a bimodal distribution of gene BMDs in both sexes, with a range of 66–104 mg/kg/day in males, and 65–94 mg/kg/day in females, beneath the lowest mode. The lowest statistically significant pathway BMD_t was LPS/IL-1 Mediated Inhibition of RXR Function, with BMD_ts of 66 and 71 mg/kg/day for males and females respectively. The lowest pathway BMD_ts with at least three genes and 5% of the pathway affected were 7.2 mg/kg bw-day for the Thyroid Hormone Metabolism II pathway in males and 3.2 mg/kg bw-day for the Acetone Degradation I pathway in females. Below we discuss the evidence supporting perturbations of the above pathways and their potential role in the toxicological effects of HBCD. We focussed our analysis primarily on DEGs found in both sexes to provide insight into mechanisms that are relevant to both males and females.

4.1. Xenobiotic metabolism and nuclear receptor activity

HBCD treatment led to the up-regulation of 14 genes involved in steroid and xenobiotic metabolism in both sexes of Fischer rats (Table 2). Moreover, xenobiotic metabolism signaling pathways were significantly altered in both sexes (Table 3). Our results suggest that HBCD increases nuclear receptor activities. For example, significant increases in the expression of *Cyp2b1* and *2b2,* which are mediated by the orphan nuclear receptor CAR, suggest CAR activation in the liver. Our results also showed that HBCD increases the expression of several PXR-mediated genes, suggesting that HBCD interacts with PXR. These results were supported by our NSC analysis showing the CAR/PXR gene set is enriched for all six HBCD treatment groups (Table S9). Moreover, two IPA pathways related to PXR and RXR were enriched in the data sets (Table 3). These results are consistent with published findings. For example, a previous study showed that HBCD exposure leads to increased expression of CAR-mediated genes in the livers of Wistar rats exposed to HBCD (Germer et al., 2006). An *in vitro* study using a stably transfected cell line showed that HBCD is an agonist of PXR (Fery et al., 2010). HBCD-induced alterations in PXR-mediated genes in the current study (both sexes) include aldehyde dehydrogenase1a1 (*Aldh1a1*) (Hartley et al., 2004), carboxylesterase 2A (*Ces2a*) (Zhang et al., 2012), *Cyp3a23/*3a1 (Ihunnah et al., 2011), and solute carrier organic anion transporter (*Slco1a4*) (Guo et al., 2002). We note that CAR and PXR signaling affects a network of genes that is involved not only in metabolism or transport of xenobiotics and endogenous substances, such as bile acid, steroids and bilirubin, but also in various physiological/pathophysiological processes such as lipid metabolism, glucose homeostasis, and inflammation. Overall, the results obtained from the current study and the companion *in vivo* study support that HBCD induces genes involved in xenobiotic metabolism, and genes regulated by CAR, PXR, and RXR, which potentially impact diverse biological processes.

Our companion paper (Gannon et al., submitted) found lower concentrations of HBCD in male versus female rats following this dietary exposure. However, a greater number of DEGs were altered in males

Table 4
Upstream Regulators identified in IPA in male and female rats following 28 day HBCD exposure.

Males

Function	Upstream Regulator	Molecule Type	Predicted Activation State	Z-score[1]	p-value	BMD_t (mkd)[‡]	$BMDL_t$ (mkd)[‡]	# genes	Target molecules in dataset
nuclear receptors	NR1I3	ligand-dependent nuclear receptor	Activated	2.4	3.4E-08	53	36	7	*ALDH1A1,Ces2a,CYP2C19,CYP3A5,EPHX1,Gstm3,Slco1a4*
	NR1I	ligand-dependent nuclear receptor	Activated	2.2	6.7E-06	53	36	6	*ALDH1A1,Ces2a,CYP2C19,CYP3A5,Gstm3,Slco1a4*
	TO-901317	chemical reagent	Activated	2.2	8.3E-05	70	45	6	*ABCG5,ABCG8,ALAS2,Ces2a,CYP3A5,EPHX1*
	HNF4A	transcription regulator	Activated	2.2	1.1E-02	73	43	13	*ABCG5,ABCG8,ALDH1A1,Ces2e,CYP3A5,DBP,EHD3,EPHA2,EPHX1,FLNA,HSD17B2,Slco1a4,TLE3*
antifibrotic activity	miR-9-5p	mature microRNA	Activated	3.1	5.9E-03	104	46	10	*AK4,ANO6,C2CD2,EXTL3,MYO10,PI4K2A,SLC13A5,SLC4A1,STEAP3,ZHX3*
	miR-133a-3p	mature microRNA	Activated	2.4	2.5E-02	114	62	6	*CCDC117,CNN2,COL1A1,NCAM2,SLC4A1,ZHX3*
suppress cell proliferation	miR-124-3p	mature microRNA	Activated	2.1	2.3E-02	108	57	11	*AK4,EHD3,EPHA2,EXTL3,FAM78A,GALNT10,MYO10,NR1D2,NYNRIN,STEAP3,ZHX3*
promote cell proliferation	miR-423-5p	mature microRNA	Activated	2.2	3.4E-02	109	61	5	*ANO6,CNN2,COL1A1,FAM222A,ZHX3*
immune response	miR-128-3p	mature microRNA	Activated	2.1	2.0E-02	112	60	8	*AK4,C2CD2,EHD3,FAM222A,FAM78A,NR1D2,PTPRB,STEAP3*
POD estimation						***104***	***46***		
suppress cell proliferation	miR-495-3p	mature microRNA	Activated	2.7	0.000288	333	230	11	*CUX1,EIF4EBP2,FAM120A,ITPK1,MOB3B,PDE8B,RCBTB1,SPICE1,ST8SIA1,TIMP2,UBE2Z*
	miR-320b	mature microRNA	Activated	2.4	0.000429	349	238	10	*CTPS1,CUX1,DIXDC1,ITPK1,MOB3B,NEK9,PLPPR1,SLC6A6,TGFBR2,UBE2Z*
	miR-218-5p	mature microRNA	Activated	2.6	0.00174	321	224	10	*ADIPOR2,CHST15,CUX1,GPAM,INSIG1,KIAA1161,ORC2,PDE8B,RCBTB1,SLC6A6*
	miR-1207-5p	mature microRNA	Activated	2.2	0.0052	367	247	8	*GAS8,GREM2,IRGQ,PPARD,SEPT9,TIMP2,UBE2Z,UPK3B*
	miR-23a-3p	mature microRNA	Activated	2.4	0.0194	354	241	9	*CHST15,CUX1,EIF4EBP2,GREM2,MFHAS1,NDST1,SPICE1,ST8SIA1,TGFBR2*
	miR-124-3p	mature microRNA	Activated	2.1	5.95E-06	370	245	19	*ADIPOR2,AHR,CPT1A,CUX1,EIF4EBP2,GPAM,GPD2,GPT2,KIAA1161,LMAN1,NDST1,NEK9,NFIC,ORC2,PER3,RAB11FIP5,SEPT9,SLC15A4,ST8SIA1*
promote cell proliferation	miR-183-5p	mature microRNA	Activated	2.4	0.00396	328	227	6	*CUX1,GPAM,GREM2,INSIG1,NDST1,SLC6A6*
	miR-221-3p	mature microRNA	Activated	2.2	0.0315	330	229	5	*CD4,CUX1,PLPPR1,ST8SIA1,TIMP2*
antifibrotic activity	miR-19b-3p	mature microRNA	Activated	2.4	0.021	328	227	9	*ABCC3,ADIPOR2,CHST15,CUX1,INSIG1,NEK9,PLPPR1,SLC6A6,TGFBR2*
	miR-9-5p	mature microRNA	Activated	2.1	0.00345	313	220	11	*CHST15,CPT1A,CUX1,DIXDC1,GPAM,INSIG1,LMAN1,PPARD,SLC6A6,TGFBR2,UBE2Z*
	let-7a-5p	mature microRNA	Activated	2.4	0.0214	357	242	9	*ADIPOR2,CTPS1,CUX1,FAM84B,IRGQ,MGLL,MOB3B,SLC25A27,ST8SIA1*
immune response	miR-130a-3p	mature microrna	Activated	3.0	0.00479	330	229	9	*CHST15,GPT2,INSIG1,ITPK1,MOB3B,NEK9,SLC6A6,TGFBR2,TIMP2*
	miR-128-3p	mature microRNA	Activated	2.2	0.0112	335	230	9	*FAM84B,GPAM,GPD2,MFHAS1,NDST1,PDE8B,PLPPR1,POFUT1,SLC6A6*
transport of glucose and bile salts	SLC13A1	transporter	Activated	2.2	1.67E-05	306	215	x	*ACTG1,GPAM,INSIG1,Mt1,UPP2*
response to oxidative stress	miR-200b-3p	mature microRNA	Activated	2.4	7.66E-05	369	248	13	*ADIPOR2,CUX1,DIXDC1,GREM2,LMAN1,MFHAS1,NDST1,NEK9,ORMDL3,PLPPR1,SLC25A27,SLC6A6,TIMP2*
coagulation	coagulation factor II	peptidase	Inhibited	-2.2	0.0018	335	231	5	*CTPS1,MFHAS1,MGLL,TGFB3,TIMP2*
	miR-1237-5p	mature microRNA	Activated	2.2	0.0234	323	224	5	*CUX1,ITPK1,KIAA1161,NEK9,SEPT9*
	miR-3194-5p	mature microRNA	Activated	2.2	0.000368	313	220	8	*ACTG1,CD4,CUX1,GAS8,GPAM,NDST1,SLC6A6,ST8SIA1*
	miR-4472	mature microRNA	Activated	2.2	0.0257	320	222	5	*CUX1,ITPK1,KIAA1161,SLC35E1,UBE2Z*

Females

Function	Upstream Regulator	Molecule Type	Predicted Activation State	z-score	p-value	BMD_t (mkd)[‡]	$BMDL_t$ (mkd)[‡]	# genes	Target molecules in dataset
liver regeneration	BMP2	growth factor	Activated	2.2	7.9E-04	111	60	5	*CYP17A1,GADD45B,IGFBP5,KLF10,MYC*
angiogenesis	Vegf	group	Inhibited	-2.4	9.5E-05	108	60	9	*ACKR3,ADAMTS1,CDC25B,CRY1,DNAJB9,INSIG1,LYVE1,MYC,SGK1*
promote cell proliferation	Hdac	group	Inhibited	-2.0	2.4E-03	106	59	4	*ADAMTS1,GADD45B,KLF10,MYC*
AHR agonist	2,4,5,2',4',5'-hexachlorobiphenyl	chemical toxicant	Activated	2.2	1.1E-05	79	50	5	*ABCC3,Cyp3a25 (includes others),GADD45B,GPX2,MYC*
PPARα agonist	pirinixic acid	chemical toxicant	Activated	2.2	2.4E-04	79	50	8	*ABCC3,CYP3A7,GADD45B,HILPDA,INSIG1,KLF10,MYC,NR1D1*
progesterone signaling	progesterone	chemical - endogenous mammalian	Inhibited	-2.1	2.0E-06	101	46	12	*ADAMTS1,ALDH1A1,ATP1B1,GABARAPL1,GSTA3,IGFBP2,IGFBP5,KLF10,MME,MYC,SGK1,TAT*
glucose and lipid metabolism	LEP	growth factor	Activated	2.4	5.5E-03	87	53	6	*ABCC3,CYP17A1,GSTA3,IGFBP2,MYC,NPR1*
resistance to cell stress	NUPR1	transcription regulator	Activated	2.4	1.2E-02	77	49	6	*ETV6,HILPDA,MYC,NR1D1,PIM1,RBMS1*
immune response	miR-381-3p	mature microRNA	Activated	2.0	4.9E-02	89	40	7	*ANKRD12,ATP1B1,GABARAPL1,GTF2E1,INSIG1,PTGFR,SLC34A2*
steroidogenesis	choriogonadotropin	complex	Inhibited	-2.1	2.0E-03	98	57	6	*ADAMTS1,CYP17A1,GTF2E1,IGFBP2,NPR1,PTGFR*

(*continued on next page*)

Table 4 (*continued*)

POD estimation							*94*	*51*		
suppress cell proliferation	miR-486-3p	mature microRNA	Activated	2.2	3.6E-02	346	241	5	*CD4,CEMIP,KCTD7,PPARD,ZNF710*
	miR-202-3p	mature microRNA	Activated	2.4	2.0E-02	350	243	6	*ADIPOR2,CYTH3,MEGF11,MSR1,STAB2,STX3*
antifibrotic activity	miR-133a-3p	mature microRNA	Activated	2.2	3.8E-02	302	217	5	*MSN,SLC6A1,STOM,UBE2Z,ZNF710*
	let-7a-5p	mature microRNA	Activated	2.3	1.0E-03	351	244	10	*ADIPOR2,CCDC141,CYTH3,MEGF11,MSR1,SLC6A1,STAB2,STX3,ZNF641,ZNF710*
endocrine disruption	daidzein	chemical drug	Inhibited	-2.0	8.2E-05	318	226	4	*CD4,DNASE1L3,ESR1,FCGR2B*
	miR-6967-5p	mature microRNA	Activated	2.2	1.0E-03	375	256	5	*HIP1,MSN,PPARD,SCUBE1,ZNF710*
	miR-3584-5p	mature microRNA	Activated	2.2	1.8E-03	375	256	5	*CD4,CD93,MFAP3,MSR1,SCUBE1*

Only upstream regulators with a p-value ≤ 0.05, and absolute z-score ≥ 2, and a minimum of four genes were included. Upstream regulators enriched in mode 1 and mode 2 are shown by white and gray colors, respectively. Median BMD_t and BMD_tL was calculated for target molecules in data sets from male and female rats. BMD_t medians for upstream regulators enriched in mode 1 were used in POD prediction. [1]Maximal fold-changes with associated FDRs across three doses were used as the input for IPA to obtain z-scores. ‡Route -adjusted $BMD_t(L)$ values in mg/kg HBCD/day in diet were converted to mg/kg-day (mkd) based on observed food intake in the rats (Anne M Gannon, Submitted).

than females herein. This could indicate the presence of more toxic metabolites in the males, but there are insufficient data to draw this conclusion at present. Our companion paper and others have shown sex-differences in HBCD response; more work is needed to determine what causes these sex-sensitivities.

4.2. Oxidative stress

HBCD altered the expression of key oxidative stress-response genes including glutathione peroxidase 2 (*Gpx2*), glutathione S-transferase alpha 3 (*Gsta3*), and *Mt1* in both male and female rats (Fig. S2). Gpx2 is involved in the detoxification of hydrogen peroxide and is an antioxidant enzyme (Trachootham et al., 2008) that inhibits oxidative stress-induced apoptotic response (Yan and Chen, 2006). Gsta3 encodes an enzyme with glutathione transferase activity whose main biological role is to protect the organism from oxidative damage (Yang et al., 2002). Mt1 participates in an array of protective stress responses and its synthesis increases during oxidative stress (Sato and Bremner, 1993). Pathway analysis of HBCD-treated livers also revealed enrichment of DEGs associated with an upstream regulator (miR-200b-3p in males) and pathway (NRF2-mediated oxidative stress response in females) involved in response to oxidative stress (Xiao et al., 2015). Thus, activation of the antioxidant defense system by HBCD suggests that this chemical increases the generation of ROS in rat livers. These findings are also consistent with previous studies reporting that HBCD causes oxidative stress and increases the levels of ROS and oxidative damage in cells in various animal models (Hu et al., 2009; Miller et al., 2016a; Wang et al., 2016b; Zhang et al., 2008b; Deng et al., 2009; An et al., 2014). For example, exposure to an environmentally relevant concentration of HBCD (0.05 mg/L) is able to induce oxidative stress in HepG2 cells (Wang et al., 2016b). Taken together, our results and the work of others (Germer et al., 2006; Miller et al., 2016a,b; van der Ven et al., 2006) support that HBCD generates oxidative stress and activates antioxidant defense systems in both male and female rat livers following dietary exposure.

4.3. Apoptosis

Enhanced production of ROS under oxidative stress conditions, if not effectively scavenged, results in oxidative damage to inter- and intra-cellular targets (e.g., DNA, proteins, lipids, and cell membranes), which leads to cell damage and death (Kehrer, 2000; Aoshima et al., 1997). A previous study reported that HBCD induces a dose-dependent increase in cellular apoptosis in HepG2 cells that is associated with HBCD-induced elevation of cellular ROS production (An et al., 2014). Another study showed that high concentrations of HBCD stimulate apoptosis in human hepatocyte L02 cells (An et al., 2013). Our results show increases in the expression of genes involved in DNA damage

Table 5
Enriched diseases or functions in male and female rats following 28 day exposure to HBCD.

Males

Categories	Diseases or Functions Annotation	p-Value	BMD_t (mkd)‡	$BMDL_t$ (mkd)‡	# genes	Molecules
Liver Proliferation	proliferation of liver cells	0.00	354	241	5	*AHR,Mt1,PPARD,TGFBR2,TIMP2*
Liver Steatosis	hepatic steatosis	0.01	328	226	5	*ADIPOR2,AHR,CPT1A,GPD2,INSIG1*
Liver Fibrosis	fibrosis of liver	0.00	342	235	4	*AHR,TGFBR2,TIMP2,TMEM67*

Females

Categories	Diseases or Functions Annotation	p-Value	BMD_t (mkd)‡	$BMDL_t$ (mkd)‡	# genes	Molecules
Liver Hyperplasia/ Hyperproliferation	liver cancer	0.03	98	58	34	*ABCC3,ADAMTS1,ADCY10,ANKRD12,CDC25B,CLIC5,CNDP1,CRY1,CYP4A22,DES,DNAJB9,GPX2, GSTA3,HTATIP2,IGFBP2,INSIG1,KLF10,LRRC49,MME,MRVI1,MX1,MYC,NR1D1,POU2F2, PPP1R3C,PRICKLE1,PTGFR,SGK1,Slco1a1,TOMM70,TWF2,TXNRD3,UPP2,ZNF202*
Liver Cholestasis	cholestasis	0.00	79	50	4	*ABCC3,GPX2,Slco1a1,Slco1a4*
Liver Necrosis/Cell Death	necrosis of liver	0.03	61	42	4	*GADD45B,MME,MYC,USP2*
Liver Inflammation/Hepatitis	inflammation of liver	0.02	336	236	4	*ADIPOR2,CCR5,ESR1,FCGR2B*

Only disease or function annotations with a p-value ≤ 0.05 and a minimum of four genes were included. Enriched diseases or functions in modes 1 and 2 are shown in white and gray shading, respectively. ‡Route -adjusted $BMD_t(L)$ values in mg/kg HBCD/day in diet were converted to mg/kg-day (mkd) based on observed food intake in the rats (Anne M Gannon et al., Submitted).

Table 6
BMD_t(L) values for the 20 genes with largest fold changes in mode 1.

Males

		low dose		medium dose		high dose		BMD_t (mkd)‡	
IDs	**Gene Symbol**	**FDR**	**FC**	**FDR**	**FC**	**FDR**	**FC**	**BMD_t**	**$BMDL_t$**
ENSRNOG00000013241	*Cyp2c13*	0.99	–1.0	0.02	**2.7**	0.00	**3.8**	66	43
ENSRNOG00000032560	*LOC100910877*	0.15	1.5	0.00	**2.5**	0.00	**3.4**	16	8
ENSRNOG00000021027	*Dbp*	0.87	–1.1	0.96	1.1	0.00	**2.9**	173	134
ENSRNOG00000011635	*Ces2e*	0.91	1.1	0.07	2.1	0.00	**2.9**	90	54
ENSRNOG00000047745	*Cyp3a23/3a1*	0.60	1.3	0.00	**2.2**	0.00	**2.8**	54	37
ENSRNOG00000013982	*Hsd17b2*	0.65	1.2	0.05	**1.5**	0.00	**2.8**	77	37
ENSRNOG00000043044	*Cnn2*	0.52	–1.5	0.02	**–2.2**	0.00	**–2.6**	44	9
ENSRNOG00000054325	*AABR07004397.2*	0.78	1.2	0.00	**1.9**	0.00	**2.6**	53	37
ENSRNOG00000000167	*Alas2*	0.57	–1.5	0.00	**–2.7**	0.00	**–2.6**	73	46
ENSRNOG00000029594	*LOC686807*	0.36	–1.7	0.02	**–2.4**	0.00	**–2.5**	114	61
ENSRNOG00000008182	*Htra3*	0.99	–1.0	0.34	–1.9	0.04	**–2.5**	129	65
ENSRNOG00000001198	*Fam222a*	0.53	–1.6	0.17	–2.1	0.02	**–2.5**	122	63
ENSRNOG00000023352	*Fam78a*	0.31	–1.7	0.05	**–2.2**	0.00	**–2.5**	173	74
ENSRNOG00000046912	*Nr1d2*	0.98	1.0	0.25	1.6	0.00	**2.4**	101	58
ENSRNOG00000030321	*LOC502176*	0.55	1.6	0.23	2.0	0.03	**2.4**	122	63
ENSRNOG00000050573	*Tgfbr3l*	0.87	1.2	0.15	2.3	0.04	**2.4**	112	60
ENSRNOG00000019058	*Gstm3*	0.37	1.5	0.01	**2.0**	0.00	**2.4**	26	6
ENSRNOG00000001484	*Gatsl2*	0.96	1.1	0.10	–2.1	0.02	**–2.3**	109	60
ENSRNOG00000024016	*Cyp2c6v1*	0.16	1.4	0.00	**2.0**	0.00	**2.3**	15	6
ENSRNOG00000000978	*Cyp3a2*	0.62	1.3	0.00	**2.4**	0.00	**2.3**	54	37
BMD_t median values								**84**	**50**

Females

		low dose		medium dose		high dose		BMD_t (mkd)‡	
IDs	**Gene Symbol**	**FDR**	**FC**	**FDR**	**FC**	**FDR**	**FC**	**BMD_t**	**$BMDL_t$**
ENSRNOG00000009329	*Nr1d1*	0.63	1.8	0.00	**4.6**	0.00	**9.7**	46	33
ENSRNOG00000008842	*Cyp4a8*	0.30	2.1	0.00	**4.9**	0.00	**4.6**	41	30
ENSRNOG00000009514	*Mme*	0.60	1.8	0.00	**3.1**	0.00	**4.6**	68	45
ENSRNOG00000019822	*Gadd45b*	0.93	1.3	0.00	**3.0**	0.00	**4.4**	49	35
ENSRNOG00000034190	*Ighm*	0.32	2.0	0.00	**2.8**	0.00	**4.0**	28	6
ENSRNOG00000013657	*Stmn3*	0.96	–1.2	0.05	**–2.0**	0.00	**–3.5**	111	63
ENSRNOG00000005341	*Upp2*	0.95	1.2	0.00	**2.3**	0.00	**3.3**	65	44
ENSRNOG00000021248	*Cdc25b*	0.93	–1.5	0.20	–2.2	0.02	**–2.8**	152	74
ENSRNOG00000007575	*Lppr1*	1.00	–1.0	0.02	**–2.1**	0.00	**–2.8**	76	49
ENSRNOG00000006663	*Usp2*	0.83	–1.5	0.00	**–3.2**	0.00	**–2.8**	55	38
ENSRNOG00000013090	*Gadd45g*	0.00	**3.8**	0.00	**3.9**	0.00	**2.7**	4	1
ENSRNOG00000026902	*Lyve1*	0.78	–1.7	0.04	**–2.4**	0.01	**–2.6**	151	73
ENSRNOG00000000969	*Cyp3a18*	0.99	1.1	0.20	1.6	0.00	**2.4**	111	63
ENSRNOG00000055530	*Panx2*	0.93	1.3	0.00	**2.1**	0.00	**2.4**	66	44
ENSRNOG00000047218	*Clic5*	0.94	–1.3	0.20	–1.7	0.00	**–2.4**	95	57
ENSRNOG00000047493	*Slco1a4*	0.50	1.4	0.00	**1.7**	0.00	**2.3**	39	13
ENSRNOG00000017206	*Igfbp5*	0.94	–1.3	0.06	–2.3	0.03	**–2.3**	115	63
ENSRNOG00000029744	*Ces2j*	0.05	**1.5**	0.00	**2.0**	0.00	**2.3**	10	3
ENSRNOG00000004425	*Klhdc1*	0.94	1.3	0.04	**2.0**	0.00	**2.2**	124	65
ENSRNOG00000056847	*Gsta3*	1.00	1.0	0.00	**1.8**	0.00	**2.1**	60	41
BMD_t median values								**65**	**44**

Male and female rats exposed to 250 (low), 1250 (medium), and 5000 (high) mg/kg HBCD/day in diet of HBCD for 28 days. ‡Route -adjusted BMD_t(L) values in mg/kg HBCD/day in diet were converted to mg/kg-day (mkd) based on observed food intake in the rats (Anne M Gannon et al., Submitted). FDR: FDR p-value; FC: Fold change.

response and apoptosis [e.g., growth arrest and DNA damage inducible beta (*Gadd45β*) in males and *Gadd45α/β/γ* in females] in rat livers. However, we note that Gadd45 proteins are implicated in the regulation of many cellular functions; thus, over-expression does not necessarily indicate apoptosis or DNA damage. Moreover, we used publicly available data to apply an NSC analysis to derive genes sets associated with DNA damage and cytotoxicity, and did not find evidence of enrichment of these gene sets in HBCD-exposed livers (Fig. 2). Likewise, *in vivo* exposure to HBCD led to increased liver weights in female Fischer rats in the absence of corresponding test article-related histopathological lesions (Gannon et al., Submitted), which is indicative of an adaptive rather than a toxic response and most likely results from the induction of hepatic xenobiotic metabolizing enzymes (Amacher et al., 1998). Taken together, neither apical nor transcriptional results in the current study support that HBCD at these doses and duration of exposure induces hepatocellular apoptosis in rats *in vivo*.

4.4. Cell cycle regulation

We found that HBCD alters the expression of genes involved in cell-division and proliferation in rat livers, including ephrin A1 (*Efna1*; up regulated in both sexes), ubiquitin specific peptidase 2 (*Usp2*; down regulated in both sexes), *Gadd45β* (up regulated in both sexes), and cell division cycle 25b (*Cdc25b*; down regulated in both sexes) (Fig. S3).

Table 7
BMD(L)$_t$s derived from Approaches #1 and #2 for male and female rats.

	Males		Females	
Approach #1	**BMD$_t$ (BMDL$_t$) (mkd)[a] [b]**		**BMD$_t$ (BMDL$_t$) (mkd)[a] [b]**	
Median of significantly enriched pathway BMD$_t$s	77	(43)	73	(47)
Median BMD$_t$s of genes from the most significantly enriched upstream regulators	104	(46)	94	(51)
20 genes with the largest fold changes	84	(50)	65	(44)
Lowest statistically significant pathway[c]	66	(43)	71	(46)

	Males		Females	
Approach #2	**BMD$_t$ (BMDL$_t$ -BMDU$_t$[d]) (mkd)[a1]**		**BMD$_t$ (BMDL$_t$ -BMDU$_t$[d]) (mkd)[a1]**	
The 1st most sensitive pathway(s) BMD$_t$s	7.2	(4.3–13)[e]	3.2	(1.3–7.6)[f]
The 2nd most sensitive pathway(s) BMD$_t$s	17	(9.4–29)[g]	6	(2.3–14)[h]
The 3rd most sensitive pathway(s) BMD$_t$s	17	(10–33)[i]	28	(12–103)[j]

[a] Route -adjusted BMD$_t$s(L) values in mg/kg HBCD/day in diet were converted to mg/kg-day (mkd) based on observed food intake in the rats (Anne M Gannon et al., Submitted).
[b] Values are in mg/kg-day.
[c] Median BMD(L)$_t$ of genes producing the lowest pathway BMD$_t$s (significantly enriched) for both males and females. Note, this pathway was LPS/IL-1 Mediated Inhibition of RXR Function in both males and females.
[d] BMDU$_t$: benchmark dose upper bound. The ability to generate a BMDU was only available in the most recent version of BMDExpress and thus was not included in Approach #1.
[e] 1st most sensitive pathway(s) in males: Thyroid Hormone Metabolism II (via Conjugation and/or Degradation).
[f] 1st most sensitive pathway(s) in females: Acetone Degradation I (to Methylglyoxal).
[g] 2nd most sensitive pathway(s) in males: Melatonin Degradation I; Nicotine Degradation II and III; Superpathway of Melatonin Degradation.
[h] 2nd most sensitive pathway(s) in females: Melatonin Degradation I; Nicotine Degradation II and III; Superpathway of Melatonin Degradation.
[i] 3rd most sensitive pathway(s) in males: Bupropion Degradation; Acetone Degradation I (to Methylglyoxal).
[j] 3rd most sensitive pathway(s) in females: PXR/RXR Activation.

Efna1 binds to its receptor and triggers downstream signals leading to inhibition of the rat sarcoma (RAS)/mitogen-activated protein kinase (MAPK) cascade, attenuates activation of MAPK by growth factor receptors, and inhibits cell proliferation (Pratt and Kinch, 2002; Novak, 2005; Miao et al., 2001). We identified multiple genes within our NGS data set (Table S11) that are linked to RAS/MAPK signaling pathways supporting previous findings of interference between HBCD and these pathways (Cato et al., 2014; Almughamsi and Whalen, 2016). Usp2 regulates diverse cellular processes by de-ubiquitination of different substrates, including key targets for tumor suppression. These target proteins for Usp2 exert their oncogenic activity predominantly by inhibiting the p53 tumor suppressor (Reichert et al., 2015). Usp2 also contributes to the regulation of other proteins involved in cell cycle, including cyclin D1 and epidermal growth factor receptor (Reichert et al., 2015; Liu et al., 2013). Gene silencing of *Usp2* affects cyclin D1 expression, leading to cell cycle arrest (Nepal et al., 2015). Gadd45β is involved in regulating proliferation and apoptosis, which can be mediated via CAR and PXR (Hernandez et al., 2009; Yamamoto et al., 2010; De Smaele et al., 2001; Locker et al., 2003). CAR/PXR activation promotes hepatocyte proliferation and suppresses apoptosis (Elcombe et al., 2014; Nakano et al., 2013). PXR-mediated overexpression of *Gadd45b* increases phosphorylation of p38 MAPK (Kodama and Negishi, 2011). MAPK families participate in complex cellular programs including proliferation, differentiation, and apoptosis (ZHANG and LIU, 2002). In addition, expression of cytoplasmic FMR-1-interacting protein 2 (*Cyfip2*) was decreased in both males and females exposed to HBCD, a gene whose inhibition has been shown to promote cell proliferation via the protein kinase B (*Akt*) signaling pathway (Jiao et al., 2017). Finally, the down-regulation of *Cdc25b* observed in our study may also contribute to cell cycle inhibition, as decreased expression of *Cdc25b* has been shown to cause cell cycle arrest (Brenner et al., 2014; Nakamura et al., 2011).

IPA upstream regulator analysis of HBCD-treated male and female livers revealed the enrichment of genes under the control of numerous important regulators involved in both the promotion and suppression of cellular proliferation including: miR-124-3p (Deng et al., 2016), miR-423-5p (Lin et al., 2011), miR-495-3p (Formosa et al., 2014), miR-320b (Wang et al., 2015), miR-218-5p (Zhu et al., 2016), miR-1207-5p (Dang et al., 2016), miR-23a-3p (Wen et al., 2016), miR-183-5p (Miao et al., 2015), and miR-221-3p (Xie et al., 2014) in males; and histone deacetylases (Hdac) (Wang et al., 2016a), miR-486-3p (Ye et al., 2016), and miR-202-3p (Zhang et al., 2014) in females (Table 4; Fig. S3). IPA disease analysis identified two functional annotations: proliferation of liver cells and liver cancer for male and female HBCD-exposed rats (Table 5). However, while HBCD isomers (α and γ) were present in both male and female livers (see companion paper), and relative liver weights were increased, histopathological evaluation revealed no evidence of hepatic hyperplasia or hypertrophy in the livers of rats exposed to technical HBCD, and traditional biochemical markers for liver damage were not elevated. We speculate that these changes are indicative of adaptive rather than toxic responses to exposure, and that a prolonged exposure may be necessary to elicit more pronounced effects (Gannon et al., Submitted). Overall, while our results suggest that HBCD triggered cell proliferation machinery in liver cells, whether this effect is adaptive or would lead to adverse effects with prolonged perturbation remains to be elucidated.

4.5. Immune response

HBCD exposure perturbed the expression of genes involved in immune response in the livers of male and female Fischer rats. Specifically, HBCD increased the transcription of several cytokine genes: a neutrophil chemoattractant [chemokine (C-X-C motif) ligand 1 (*Cxcl1*)] and T-cell chemoattractant (*Cxcl9*) in males, and a macrophage chemoattractant (*Cxcl14*), in females. The liver has an essential role in immune responses and because of an abundance of liver-specific Kupffer cells, natural killer (NK) cells, and natural killer T (NKT) cells and their rapid responses to stimuli, the liver is considered to be an organ with innate immune features (Robinson et al., 2016; Dong et al., 2007; Bilzer et al., 2006). Up-regulation of cytokines in our study

suggests that HBCD activates immune responses in the liver and, more specifically, the Kupffer cells. However, in contrast, *Cd4* and *Cd5l* expression was significantly decreased in both male and female rats. Cd4 is a glycoprotein that is on the surface of immune cells and plays a critical role in the development and function of the immune system (Bowers et al., 1997). *Cd5l* is mainly expressed by macrophages in inflamed tissues and is a key protein in the control of immune homeostasis and inflammatory disease (Sanjurjo et al., 2015). A previous study showed that HBCD increases secretion of the inflammatory cytokine interferon gamma (IFN-γ), decreases the expression of cell surface proteins (e.g., Cd16 and Cd56), and decreases the cytolytic ability of human Natural killer (NK) cells (Almughamsi and Whalen, 2016; Hinkson and Whalen, 2009). Hinkson and Whalen (2010) suggested that the inability of human NK cells to lyse target cells is due to decreases in the expression of cell surface proteins (Hinkson and Whalen, 2010). Our companion paper revealed that *in vivo* exposure to HBCD targets the peripheral immune system, which showed evidence of adverse effects, particularly in male Fischers, although female rats were also affected (Gannon et al., Submitted). Decreases in the density and area of the follicles, PALS, and marginal zones were seen, coupled with lower levels of splenocyte proliferation both in the presence and absence of challenge, suggesting a diminishing effect on the adaptive immune response. Moreover, decreases in the T/B cell ratio was evident in blood lymphocyte populations due to declines in both helper and cytotoxic T cell populations and increases in B cells. Additionally, monocytes, total protein levels, and NK cells were increased in treated animals. Taken together, these events are indicative of an inflammatory response (Heymann et al., 2015). Although alterations in the expression of key immune response genes and the results from *in vivo* study suggest that HBCD affects immune response, more work is needed to further clarify the toxicological outcome of this perturbation.

4.6. Liver weight

HBCD-exposed females in our companion paper exhibited dose-dependent increases in liver weight (Gannon et al., Submitted). HBCD-induced increases in liver weight have also been observed in both male and female rats, and mice, in other studies (Yanagisawa et al., 2014; Gannon et al., Submitted; van der Ven et al., 2006; Zeller and Kirsch, 1969, 1970; Chengelis, 1997). It has been suggested that increased liver weight following xenobiotic exposure is associated with increased synthesis of enzymes and transport molecules to inactivate, conjugate, and transport xenobiotics in order to increase the detoxification capacity of the liver (Maronpot et al., 2010). As discussed above, our results clearly show that HBCD activates xenobiotic metabolism. BMD analysis for common xenobiotic genes in both sexes showed a lower BMD mean value for males than females, suggesting the activation of xenobiotic metabolism in liver of HBCD-exposed rats occurs at a lower dose in males than females (Table 2). This is also consistent with others who found sex differences in response to HBCD exposure, with females exhibiting larger effects on liver weight, which may be offset by adaptive responses in the livers of males (Chengelis, 2001; Germer et al., 2006; Miller et al., 2016a; van der Ven et al., 2006, 2009; Gannon et al., Submitted). Recent studies suggest that many xenobiotic compounds increase liver weight through a common mechanism of action involving activation of the nuclear hormone receptors CAR, PXR, or PPARα (Maronpot et al., 2010). For example, a xenobiotic activator of CAR increases induction of *Gadd45b,* leading to the *de novo* proliferation and rapid expansion of liver mass to protect against xenobiotic insults (Tian et al., 2011). Indeed, $CAR^{-/-}$ animals show no increase in liver mass after treatment with CAR ligands (Wei et al., 2000), indicating the necessity of this gene. Our results are consistent with this, as described above; signature analysis of HBCD-exposed rat livers was consistent with activation of CAR/PXR and we found significant increases *Gadd45b* expression. Finally, the expression of several transporter genes that are involved in carrying xenobiotics and bile acid were increased (Table S3). Taken together, our gene expression results suggest that HBCD induces liver weight increases through these previously identified mechanisms (Wei et al., 2000; Tian et al., 2011; Maronpot et al., 2010), providing mechanistic insight into this phenomenon (Fig. S4).

4.7. Metabolism of glucose and lipids

Global transcriptional profiling of liver tissues from HBCD-treated male and female rats confirms previous studies (Zeller and Kirsch, 1970; Wang et al., 2016b; Yanagisawa et al., 2014) showing that HBCD disturbs the metabolism of glucose and lipids. The results of a previous study on rats exposed to HBCD for 7 days showed significant alterations in the abundance of lipid metabolism-related proteins like mitochondrial d-beta-hydroxybutyrate dehydrogenase (Bdh; which is involved in ketone body metabolism), 3-ketoacyl-CoA thiolase (Thim; which is involved in the pathway fatty acid metabolism), Pyruvate kinase PKLR (Kpyr; which plays a key role in glycolysis), and Hydroxymethylglutaryl-CoA synthase (Hmcs2; which is involved in cholesterol biosynthesis) (Miller et al., 2016a,b).

Our results also suggest that HBCD has adipogenic activity. The expression of Insulin-induced genes 1 (*Insig1*) and *Pparδ*, which both have inhibitory effects on lipogenic gene expression, was significantly decreased in male and female rats. A low level of Insig1 protein leads to the transcription of genes required for lipogenesis, cholesterol synthesis, and glucose homeostasis in diverse tissues including liver (Dong and Tang, 2010). Moreover, Insig1 increases ubiquitin-mediated degradation of 3-hydroxyl-3-methylglutaryl-coenzyme A (HMG-CoA) reductase, which is involved in the metabolic pathway that produces cholesterol (Dong and Tang, 2010). Although alteration in HMG-CoA reductase expression was not detected in the current study, a previous study (Miller et al., 2016a) showed that the abundance of Hmcs2 protein significantly decreased following HBCD exposure. Hmcs2 is an enzyme that synthesises HMG-CoA, which is the substrate for HMG-CoA reductase. Pparδ induces *Insig1* and inhibits activation of sterol regulatory element-binding proteins (SREBPs) processing into the mature form, which results in suppression of lipogenic gene expression (Qin et al., 2008) and hepatic lipogenesis in obese diabetic mice (Qin et al., 2008) (Fig. S5). Overall, decreased expression of *Insig1* and *Pparδ* in both male and female rats by HBCD may be indicative of transcriptional activation of lipogenic genes in hepatocytes.

In addition to the above, HBCD altered the expression of other genes involved in lipid metabolism (Fig. S5). A significant decrease in the expression of adiponectin receptor (*Adipor2*) was observed in both sexes. Adiponectin stimulates AMPK signaling, switching cells from active ATP consumption (e.g., fatty acid and cholesterol biosynthesis) to active ATP production (e.g., fatty acid and glucose oxidation). Down-regulation of *Adipor2* is associated with diet-induced liver steatosis in mice (Peng et al., 2009), and inhibition of *Adipor2* signaling in C57BL/6 mouse liver leads to decreased expression of acyl-CoA oxidase (*Aco*), which is involved in lipid metabolism (Tomita et al., 2008). We also observed an increase in the expression of *Aldh1a1* in both males and females in the high HBCD dose group (Fig. S6). Aldh1a1 plays an important role in gluconeogenesis and lipid metabolism. *Aldh1a1*-null mice resist obesity following administration with a high-fat diet (Yang et al., 2012). *In vitro*, *Aldh1a1* is increased during adipocyte differentiation and *Aldh1a1*-deficient adipocytes have impaired adipogenesis compared with wild-type adipocytes due to dramatic decreases in *Pparγ* expression (Reichert et al., 2011). Primary hepatocytes isolated from *Aldh1a1*-null mice have significantly lower levels of triacylglycerol synthesis compared to wild type mice (Kiefer et al., 2012). Aldh1a1 converts retinaldehyde (Rald) to retinoic acid (RA) (Duester et al., 2003; Petrosino et al., 2014) and the impact of Aldh1a1 on adipogenesis is linked to its key role in RA production during adipogenesis (Reichert et al., 2011). In our study, various other genes that are involved in lipid metabolism were also perturbed including: *Cd5l,* glycerol-3-phosphate dehydrogenase 2 (*Gpd2),* alcohol dehydrogenase 6

(*Adh6*), and *Adh7* and are discussed in more detail in supplementary materials. Taken together, our results suggest that HBCD alters the expression of key lipid metabolism genes and perturbs the retinoid signaling pathway, which may lead to increased adipogenesis in rat liver.

HBCD exposure also caused an increase in the expression of carnitine palmitoyltransferase I (*Cpt1a;* which is involved in lipid oxidation) in both male and female rats. Cpt1a initiates the mitochondrial oxidation of long-chain fatty acids. Increased expression of *Cpt1a* may provide energy for cells to respond to the xenobiotic challenge, or may help cells to dispose of surplus fatty acids.

While the apical data generated in our previous study do not explicitly support or confirm altered lipid metabolism or *de novo* adipogenesis, we note increased body weight relative to controls in the highest dose group throughout the parallel study in female Fischers (Gannon et al., Submitted) and previous studies (Ema et al., 2008; Heindel et al., 2015). The length of exposure in this study may well be insufficient to result in the manifestation of overt changes in lipid metabolism; however, the gene expression deviations seen here coupled with the body weight changes could be early predictors of imminent adverse effects that culminate in increased adipogenesis. Overall, our results show that HBCD exposure alters the expression of lipid metabolism genes in rat livers, suggesting that HBCD has the potential to alter metabolic and lipid homeostasis, and liver adipogenesis. This novel mechanism warrants further research at the phenotypic level to confirm that this pathway is perturbed and to determine the long-term consequences of these effects on the liver and organism.

4.8. Disruption in hormonal balance

It is well established that HBCD exposure perturbs the thyroid axis, causing decreases in triiodothyronine (T_3) and thyroxine (T_4) levels, and increases in thyroid stimulating hormone (TSH) and thyroid gland weight (Marvin et al., 2011; Miller et al., 2016a; Palace et al., 2008, 2010; Saegusa et al., 2009; Canton et al., 2008; van der Ven et al., 2006; Yamada-Okabe et al., 2005; Chengelis, 2001; Gannon et al., Submitted; Ema et al., 2008). Previous work *in vivo* and *in vitro* demonstrated that microsomal enzyme inducers in general cause increases in metabolism and excretion of thyroid hormone (TH), which is followed by increases in TSH (Vansell and Klaassen, 2002; Hood and Klaassen, 2000). Glucuronidation by hepatic uridine 5′-diphospho-glucuronosyltransferase (UDP)-glucuronosyltransferase (UGT) is one of the major metabolic pathways of T3 and T4 (Visser et al., 1993; Saito et al., 1991; Yamanaka et al., 2007), increases of which lead to increased biliary elimination of the conjugated hormone (Barter and Klaassen, 1992; Vansell and Klaassen, 2002). UGT isomers differ in their glucuronidation activities; for example, an *in vitro* study showed that *Ugt1a8* catalyzes T3 and T4 glucuronidation with activity levels as much as 8- and 4-fold higher than other UGT isoenzymes, respectively (Richardson and DeVito, March 16–20, 2008). Our data support that HBCD activates nuclear receptors in liver, initiating transcription of xenobiotic metabolizing enzymes that could increase metabolism and excretion of TH. Moreover, increases occurred in *Ugt1a8* (1.7-fold and 1.8-fold in males and females, respectively), *Ugt2a1* (2.3-fold in males and 1.9-fold in females) and *Ugt2b17* (2.8-fold in males) in liver tissues of rats exposed to the highest dose of HBCD. If these changes are also consistent with increased enzymatic activity in liver, this could translate into increased hepatic T3 and T4 glucuronidation and increased biliary elimination. We have also demonstrated that treatment with HBCD resulted in increased thyroid weight in the two highest doses relative to controls in male Fischer rats, decreased total T4 (in males) and a decrease in female Fischer total T4 levels that approached significance ($p = 0.056$), and that the changes in circulating hormones are reflective of the hypertrophy and colloid depletion that was reported in all strains tested in a dose-dependent manner (Gannon et al., Submitted). Others have also shown that disruption of thyroid homeostasis is a primary toxic effect of other BRFs (Birnbaum and Staskal, 2004). Overall, the results of our study suggest that HBCD perturbs the thyroid axis by increasing the expression of xenobiotic metabolism genes and we note that in males the Thyroid Hormone Metabolism II pathway had the lowest BMD_t.

In addition to alterations in thyroid hormone levels, HBCD exposure increased *Cyp3a2* expression in both males and females. This enzyme catalyzes the conversion of testosterone to 6-beta-hydroxytestosterone. HBCD-exposed female rats also exhibited increased expression of two male-specific genes, *Cyp2c11* and *Cyp2c13* (Waxman and Holloway, 2009) that both metabolize testosterone. Previous work confirms that chemicals perturb hormone regulation by induction of hepatic steroid-metabolizing enzymes (LeBlanc and Waxman, 1988, 1990; Chang and Waxman, 1993)(Birnbaum and Staskal, 2004). In all, our data suggest a disruption in hormone regulation, the effects of which are far reaching and potentially extend beyond the exposure period given that small but significant changes to pituitary and thyroid hormone signaling can result in transgenerational changes if those perturbations occur during critical points in development.

4.9. Fibrotic versus anti-fibrotic effects

Gene expression profiles from the HBCD-exposed rats in our study are consistent with potential anti-fibrotic activity. To investigate this more deeply, we compared our data to a published adverse outcome pathway (AOP) for liver fibrosis (Horvat et al., 2017; Landesmann, 2016) (Fig. S7). As described above, we found that HBCD-induced transcriptional changes were suggestive of hepatocyte injury, apoptosis, oxidative stress, and immune reactions (which are also key events in the AOP for liver fibrosis). Therefore, HBCD-induced toxicity may include hepatic fibrosis. However, there was no evidence of fibrosis observed by Gannon et al. (Gannon et al., Submitted). Our data show that HBCD exposure led to decreased expression of moesin (*Msn*) and connective tissue growth factor (*Ctgf*), suggesting that HBCD suppresses hepatic stellate cell (HSC) activity. HSC activation is a critical event in hepatic fibrosis. Msn-deficient mice display impaired HSC migration, reduced collagen deposition, and decreased fibrosis in response to injury (Okayama et al., 2008). Silencing *Ctgf* expression inhibits HSC activation and prevents liver fibrosis in rats (Li et al., 2006). Previous studies have also shown that Msn, Ctgf, actin gamma 1 (Actg1), and myosin-heavy chain 10 (Myh10) promote collagen and extracellular matrix (ECM) accumulation (Lipson et al., 2012; Dooley and ten Dijke, 2012; Okayama et al., 2008). Therefore, significant decreases in the expression of these genes observed in the current study also suggest that HBCD suppresses collagen and ECM accumulation. In addition, the expression of heat shock protein 70 (*Hsp70*) Member 4 Like (*Hspa4l*) was decreased in both males and females. Suppression of *Hsp70* expression using siRNAs results in a decrease in collagen production in keloid fibroblasts compared with controls (Shin et al., 2015). In addition to the above genes, the expression of several pro-fibrogenic genes was significantly decreased in males, including collagen proteins (*Col1a1, Col13a1,* and *Col4a2*). Thus, we suggest that following HBCD exposure in liver, there is a balance between induction of processes consistent with fibrosis that are offset by potential suppression of processes responsible for the accumulation of collagen and deposition of ECM, a critical key event in liver fibrosis (Vinken, 2013; Willett et al., 2014).

4.10. Circadian rhythm

Circadian rhythms are internal clocks in the body that regulate a wide array of daily physiological functions (e.g., sleep patterns, hormonal control, metabolism, and immune response (Masri and Sassone-Corsi, 2013)). Disruption of circadian rhythm genes can profoundly perturb physiological and biological functions (Eckel-Mahan and Sassone-Corsi, 2013; Scheiermann et al., 2013), and increase the risk of several diseases including obesity, endocrine disruption,

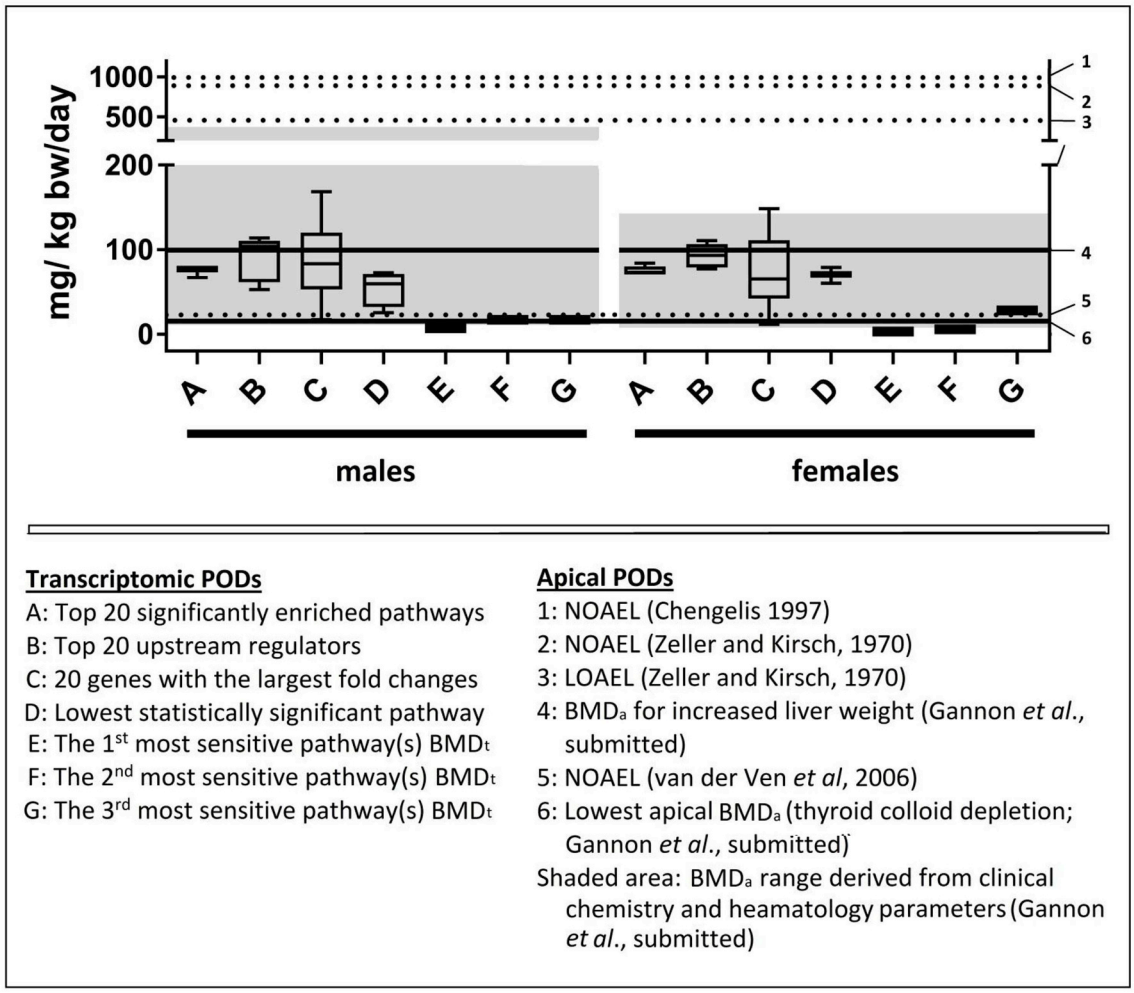

Fig. 4. Apical PODs are shown using dashed lines (previous studies) and solid lines (Gannon et al., Submitted). *(1)* NOAEL of 1000 mkd based on increased liver weights and severity of colloid loss in the thyroid glands of rats administered HBCD by oral gavage for 28 days (Chengelis, 1997); *(2* and *3)* LOAEL and NOAEL of 450 and 925 mkd based on increased absolute and relative liver weights and thyroid follicular hyperplasia (Zeller and Kirsch, 1970); *(4)* BMD_a of 99.5 mkd obtained for increased liver weight (Gannon et al., Submitted); *(5)* NOAEL of 22.9 mkd based on liver enzyme induction (van der Ven et al., 2006); *(6)* the lowest BMD_a value of 15.6 mkd derived from increased incidence of thyroid colloid depletion (Gannon et al., Submitted); *shaded areas* indicate the range of BMD_as obtained from clinical chemistry and haematology parameters (Gannon et al., Submitted). Transcriptional PODs derived using four different gene list: *(A)* median of significantly enriched pathway BMD_ts; *(B)* median BMD_ts of genes from the most significantly enriched upstream regulators; *(C)* 20 genes with the largest fold changes; *(D)* lowest significant pathway BMD_t (Thomas et al., 2013b); *(E-G)* the lowest (i.e., 'most sentitive') pathway BMD_ts with at least three genes and 5% of the pathway affected.

neurodegenerative disorders, and cancer (Froy, 2010; Musiek, 2015; Tsang et al., 2013; Sahar and Sassone-Corsi, 2009; Savvidis and Koutsilieris, 2012). Mammalian circadian rhythms are generated by a feedback loop in which clock circadian regulator (*Clock*) and AHR nuclear translocator like (*Bmal1*) form a heterodimer to activate period circadian clock (*Per*) and cryptochrome circadian clock (*Cry*) transcription. Increased Per and Cry proteins act as transcriptional repressors that decrease the transcriptional activity of Clock and Bmal1 (Ye et al., 2014). In addition to Per and Cry, Nr1d1 and Nr1d2 have been proposed to form an accessory feedback loop that contributes to clock function (Cho et al., 2012). For example, overexpression of *Nr1d1* is an effective genetic tool to silence circadian function (Partch et al., 2014). Usp2 regulates Per1 function and it was shown that mice devoid of *Usp2* display defects in clock function (Yang et al., 2014). Our study shows that HBCD treatment alters the expression of several genes involved in circadian rhythm (Fig. S6). These genes are critical to proper regulation of glucose and lipid metabolism, sleep, and energy balance. We observed significant increases in the expression of *Per3, Nr1d1,* and *Nr1d2,* and significant decreases in the expression of *Cry1* and *Usp2* in male and female rats. HBCD-induced increases in the expression of *Per3* and *Nr1d1/2*, and decreases in *Usp2*, may lead to repressed circadian transcriptional activities driven by Clock and Bmal1. A growing body of evidence indicates that environmental chemicals can disrupt circadian rhythms. For example, a recent study also showed acrylamide-induced circadian gene oscillation disorder and blocked circadian-related protein in mouse livers and in HepG2 cells (Tan et al., 2018). It is established that xenobiotics can influence circadian rhythms through regulation of circadian gene expression (Claudel et al., 2007) and our study suggests that HBCD is one of these xenobiotics.

4.11. Synopsis of molecular alterations that may impact health

The results obtained from the NSC analysis for HBCD are in agreement with previous studies pointing to a molecular initiating event that involves the interaction of HBCD with CAR/PXR signaling that may lead to several adverse effects. Moreover, the results of the NSC analysis do not support the induction of genotoxicity or carcinogenicity by HBCD, and published *in vitro* and *in vivo* genotoxicity tests for HBCD are negative. CAR/PXR activation and enzyme induction in the liver by HBCD likely leads to increased metabolism of thyroid hormones, which could play a role in the observed effects on thyroid in apical studies. In addition, our data suggest that HBCD exposure disturbs the metabolism

of glucose and lipids in the livers of both male and female rats, and that it may have adipogenic activity. We also found perturbations in pathways consistent with the induction of fibrosis, which appear to be offset by gene expression changes that are consistent with anti-fibrotic effects. Thus, two novel effects (i.e., adipogenesis and fibrotic activities) for HBCD that are predicted based on transcriptomic data in this study warrant further investigation.

4.12. Derivation of a transcriptional point of departure

Transcriptional PODs may serve as predictors of the doses at which adverse effects occur (Farmahin et al., 2016; Thomas et al., 2007, 2011, 2013b; Moffat et al., 2015). A variety of approaches have been proposed for the use of toxicogenomics to inform chemical MOA and POD (Thomas et al., 2007, 2013a; Bourdon-Lacombe et al., 2015; Jackson et al., 2014; Firestone et al., 2010; Hester et al., 2015; Farmahin et al., 2016). Below we compare PODs derived from apical analyses to our transcriptional profiling.

4.12.1. Apical POD

Analysis of all apical data in our cohort study (Gannon et al., Submitted) revealed that BMD_as for clinical chemistry and haematology parameters spanned from 11.4 mkd to 371.4 mkd in males, and 9.5 mkd to 244.5 mkd in females. For comparison with our transcriptional BMD_ts, we selected the BMD_a for increased liver weight in female rats (99.5 mkd) on the same strain of rats (Gannon et al., Submitted) as a general metric of adverse effects to liver. In addition, histological and organ weight changes in these Fischer rats were considered, as these endpoints are typically used in POD derivation in risk assessment. Of these measures, the lowest BMD_a value was 15.6 mkd for increased incidence of thyroid colloid depletion in males (Fig. 4). Thus, we also contrasted our BMD_ts against this apical endpoint, as effects on thyroid hormones were predicted based on the liver gene expression analysis. Comparative POD_a values for HBCD in other studies range from 22.9 mkd to 1000 mkd (Fig. 4) (Zeller and Kirsch, 1970; Chengelis, 1997; van der Ven et al., 2006).

4.12.2. Transcriptional PODs

Transcriptional BMD_ts showed a bi-modal distribution in both males and females. To be conservative, we derived the BMD_ts below from mode 1 of the gene BMD_t distribution. The median BMD_t values for significantly enriched pathways, upstream regulators, the 20 genes with the largest FC, and the lowest pathway BMD_t of the significantly enriched pathways in mode 1 ranged from 66 to 104 mkd in males, and 65 to 94 mkd in females (Table 7). The median BMD_ts for both males and females were 4- to 7-fold higher than the thyroid colloid depletion BMD_a (all BMD_t were higher than the BMD_a), and 1- to 1.5-fold lower than the BMD_a for liver weight increase in our parallel study.

Very recently, after completion of our transcriptomic BMD analysis (Approach #1), the US National Toxicology Program released the outcome of an expert panel examining their proposed approach to genomic BMD modeling (NTP, 2018). BMDExpress was subsequently updated (BMDExpress 2.3) to implement these recommendations. Therefore, we re-analyzed our transcriptomic data to derive the lowest BMDs for males and females that have at least three genes and 5% of the pathway modeled as per these recommendations, as well as implementing the other modifications (e.g., alterations to filtering parameters and number of models used). We refer to these as the three overall most sensitive gene-sets (pathways) in both sexes. The lowest of these BMD_t values were 7.2 and 3.2 mg/kg bw-day for males and females, respectively. These are within the same range (marginally lower) as the lowest BMD_a values derived from analysis of apical data in our cohort study (13.7 and 9.6 mg/kg bw-day in males and females, respectively). Thus, within this study, the BMD_t values derived from the NTP's approach are the most conservative transcriptomic POD. This dose reflects the dose below which there is likely to be no biological activity in the target organs (NTP, 2018).

The differences between the BMD_t values derived from these two approaches show the importance of pre-filtering to BMD analysis outcome (Fig. 4). Stringent filtering methods will minimize the effect of background noise and/or obtaining an overprotective BMD_t value, but may also reduce the number of discoveries, potentially reducing the probability of detecting some responsive genes. Stringent filtering methods may also lead to a transcriptomic BMD_t value greater than the lowest apical BMD_a (but not always, please see Webster et al., 2015). Conversely, using less stringent filtering methods may lead to overly conservative BMD_ts. In this example, our BMD_ts are not overly conservative as they are aligned with the lowest apical BMD_ts. Thus, such an approach would be the most protective and useful when the goal is to determine margins to assess whether further evaluation is required. Overall, the results support that BMD_ts derived from transcriptomic analyses can be used as PODs for risk assessment (Fig. 4).

5. Conclusions

Our toxicogenomic data suggest that HBCD perturbs various biological processes including metabolism of xenobiotic, activation of nuclear receptors, oxidative stress, cell-division cycle, metabolism of glucose and lipid, circadian regulation, immune responses, fibrotic activity, and hormonal balance in both male and female rats. While HBCD clearly shows gender-specific differences in gene expression, it generally perturbs similar biological processes, and yields similar BMD_ts, in both males and females. Statistical analysis of transcriptional profiles suggests that HBCD interacts with PXR/CAR and is not genotoxic. The most significant pathways, upstream regulators, and the largest changing genes had median BMD_ts for both males and females within the range (generally within less than 5-fold) of previously published PODs derived from traditional toxicity. The lowest pathway with at least three genes and 5% of the pathway affected yielded somewhat more conservative BMD_t values that approximated the BMD_a values of the lowest apical endpoints. This study lends support to the utility of toxicogenomics to (1) identify chemical pathway perturbations and potential toxicological hazards; (2) provide insight into MOA; and (3) estimate a POD for risk assessment.

Appendix A. Supplementary data

Supplementary data to this article can be found online at https://doi.org/10.1016/j.fct.2018.12.032.

Transparency document

Transparency document related to this article can be found online at https://doi.org/10.1016/j.fct.2018.12.032.

References

Alaee, M., Arias, P., Sjodin, A., Bergman, A., 2003. An overview of commercially used brominated flame retardants, their applications, their use patterns in different countries/regions and possible modes of release. Environ. Int. 29, 683–689 S0160-4120(03)00121-1.

Almughamsi, H., Whalen, M.M., 2016. Hexabromocyclododecane and tetrabromobisphenol A alter secretion of interferon gamma (IFN-gamma) from human immune cells. Arch. Toxicol. 90, 1695–1707. https://doi.org/10.1007/s00204-015-1586-6.

An, J., Chen, C., Wang, X., Zhong, Y., Zhang, X., Yu, Y., Yu, Z., 2014. Oligomeric proanthocyanidins alleviate hexabromocyclododecane-induced cytotoxicity in HepG2 cells through regulation on ROS formation and mitochondrial pathway. Toxicol. In. Vitro. 28, 319–326. https://doi.org/10.1016/j.tiv.2013.11.009.

An, J., Zou, W., Chen, C., Zhong, F.Y., Yu, Q.Z., Wang, Q.J., 2013. The cytological effects of HBCDs on human hepatocyte L02 and the potential molecular mechanism. J. Environ. Sci. Health. A. Tox. Hazard. Subst. Environ. Eng. 48, 1333–1342. https://doi.org/10.1080/10934529.2013.781875.

Aoshima, H., Satoh, T., Sakai, N., Yamada, M., Enokido, Y., Ikeuchi, T., Hatanaka, H., 1997. Generation of free radicals during lipid hydroperoxide-triggered apoptosis in PC12h cells. Biochim. Biophys. Acta 1345, 35–42 S0005-2760(96)00159-2.

Barghi, M., Shin, E., Son, M., Choi, S., Pyo, H., Chang, Y., 2016.

Hexabromocyclododecane (HBCD) in the Korean food basket and estimation of dietary exposure. Environ. Pollut. 213, 268–277. https://doi.org/10.1016/j.envpol.2016.02.026.
Barter, R.A., Klaassen, C.D., 1992. UDP-glucuronosyltransferase inducers reduce thyroid hormone levels in rats by an extrathyroidal mechanism. Toxicol. Appl. Pharmacol. 113, 36–42.
Berger, R.G., Lefevre, P.L., Ernest, S.R., Wade, M.G., Ma, Y.Q., Rawn, D.F., Gaertner, D.W., Robaire, B., Hales, B.F., 2014. Exposure to an environmentally relevant mixture of brominated flame retardants affects fetal development in Sprague-Dawley rats. Toxicology 320, 56–66. https://doi.org/10.1016/j.tox.2014.03.005.
Bilzer, M., Roggel, F., Gerbes, A.L., 2006. Role of Kupffer cells in host defense and liver disease. Liver Int. 26, 1175–1186 LIV1342.
Bourdon-Lacombe, J.A., Moffat, I.D., Deveau, M., Husain, M., Auerbach, S., Krewski, D., Thomas, R.S., Bushel, P.R., Williams, A., Yauk, C.L., 2015. Technical guide for applications of gene expression profiling in human health risk assessment of environmental chemicals. Regul. Toxicol. Pharmacol. 72, 292–309. https://doi.org/10.1016/j.yrtph.2015.04.010.
Bowers, K., Pitcher, C., Marsh, M., 1997. CD4: a co-receptor in the immune response and HIV infection. Int. J. Biochem. Cell Biol. 29, 871–875 S1357-2725(96)00154-9.
Brenner, A.K., Reikvam, H., Lavecchia, A., Bruserud, O., 2014. Therapeutic targeting the cell division cycle 25 (CDC25) phosphatases in human acute myeloid leukemia–the possibility to target several kinases through inhibition of the various CDC25 isoforms. Molecules 19, 18414–18447. https://doi.org/10.3390/molecules191118414.
Cai, H., Chen, H., Yi, T., Daimon, C.M., Boyle, J.P., Peers, C., Maudsley, S., Martin, B., 2013. VennPlex–a novel Venn diagram program for comparing and visualizing datasets with differentially regulated datapoints. PLoS One 8, e53388. https://doi.org/10.1371/journal.pone.0053388.
Canton, R.F., Peijnenburg, A.A., Hoogenboom, R.L., Piersma, A.H., van der Ven, L.T., van den Berg, M., Heneweer, M., 2008. Subacute effects of hexabromocyclododecane (HBCD) on hepatic gene expression profiles in rats. Toxicol. Appl. Pharmacol. 231, 267–272. https://doi.org/10.1016/j.taap.2008.04.013.
Cato, A., Celada, L., Kibakaya, E.C., Simmons, N., Whalen, M.M., 2014. Brominated flame retardants, tetrabromobisphenol A and hexabromocyclododecane, activate mitogen-activated protein kinases (MAPKs) in human natural killer cells. Cell Biol. Toxicol. 30, 345–360. https://doi.org/10.1007/s10565-014-9289-y.
Chang, T.K., Waxman, D.J., 1993. Cyclophosphamide modulates rat hepatic cytochrome P450 2C11 and steroid 5 alpha-reductase activity and messenger RNA levels through the combined action of acrolein and phosphoramide mustard. Cancer Res. 53, 2490–2497.
Chengelis, C.P., 2001. A 90-day Oral (Gavage) Toxicity Study of HBCD in Rats. , WIL-186012. Wil Reseach Laboratories, Ashland, OH, U.S.A, pp. 1527.
Chengelis, C.P., 1997. A 28-day Repeated Dose Oral Toxicity Study of HBCD in Rats. Wil Research Laboratories, Inc., Ashland, OH Laboratory Study No. WIL-186004.
Cho, H., Zhao, X., Hatori, M., Yu, R.T., Barish, G.D., Lam, M.T., Chong, L., DiTacchio, L., Atkins, A.R., Glass, C.K., Liddle, C., Auwerx, J., Downes, M., Panda, S., Evans, R.M., 2012. Regulation of circadian behaviour and metabolism by REV-ERB-a and REV-ERB-ß. Nature 485, 123–127. https://doi.org/10.1038/nature11048.
Claudel, T., Cretenet, G., Saumet, A., Gachon, F., 2007. Crosstalk between xenobiotics metabolism and circadian clock. FEBS Lett. 581, 3626–3633. https://doi.org/10.1016/j.febslet.2007.04.009.
Dang, W., Qin, Z., Fan, S., Wen, Q., Lu, Y., Wang, J., Zhang, X., Wei, L., He, W., Ye, Q., Yan, Q., Li, G., Ma, J., 2016. miR-1207-5p suppresses lung cancer growth and metastasis by targeting CSF1. Oncotarget 7, 32421–32432. https://doi.org/10.18632/oncotarget.8718.
Davis, J.A., Gift, J.S., Zhao, Q.J., 2011. Introduction to benchmark dose methods and U.S. EPA's benchmark dose software (BMDS) version 2.1.1. Toxicol. Appl. Pharmacol. 254, 181–191. https://doi.org/10.1016/j.taap.2010.10.016.
De Smaele, E., Zazzeroni, F., Papa, S., Nguyen, D.U., Jin, R., Jones, J., Cong, R., Franzoso, G., 2001. Induction of gadd45beta by NF-kappaB downregulates pro-apoptotic JNK signalling. Nature 414, 308–313. https://doi.org/10.1038/35104560.
Deng, D., Wang, L., Chen, Y., Li, B., Xue, L., Shao, N., Wang, Q., Xia, X., Yang, Y., Zhi, F., 2016. MicroRNA-124-3p regulates cell proliferation, invasion, apoptosis, and bioenergetics by targeting PIM1 in astrocytoma. Cancer Sci. 107, 899–907. https://doi.org/10.1111/cas.12946.
Deng, J., Yu, L., Liu, C., Yu, K., Shi, X., Yeung, L.W., Lam, P.K., Wu, R.S., Zhou, B., 2009. Hexabromocyclododecane-induced developmental toxicity and apoptosis in zebrafish embryos. Aquat. Toxicol. 93, 29–36. https://doi.org/10.1016/j.aquatox.2009.03.001.
Dobin, A., Davis, C.A., Schlesinger, F., Drenkow, J., Zaleski, C., Jha, S., Batut, P., Chaisson, M., Gingeras, T.R., 2013. STAR: ultrafast universal RNA-seq aligner. Bioinformatics 29, 15–21. https://doi.org/10.1093/bioinformatics/bts635.
Dong, X.Y., Tang, S.Q., 2010. Insulin-induced gene: a new regulator in lipid metabolism. Peptides 31, 2145–2150. https://doi.org/10.1016/j.peptides.2010.07.020.
Dong, Z., Wei, H., Sun, R., Tian, Z., 2007. The roles of innate immune cells in liver injury and regeneration. Cell. Mol. Immunol. 4, 241–252.
Dooley, S., ten Dijke, P., 2012. TGF-beta in progression of liver disease. Cell Tissue Res. 347, 245–256. https://doi.org/10.1007/s00441-011-1246-y.
Duester, G., Mic, F.A., Molotkov, A., 2003. Cytosolic retinoid dehydrogenases govern ubiquitous metabolism of retinol to retinaldehyde followed by tissue-specific metabolism to retinoic acid. Chem. Biol. Interact. 143–144, 201–210 S0009279702002041.
Eckel-Mahan, K., Sassone-Corsi, P., 2013. Metabolism and the circadian clock converge. Physiol. Rev. 93, 107–135. https://doi.org/10.1152/physrev.00016.2012.
Elcombe, C.R., Peffer, R.C., Wolf, D.C., Bailey, J., Bars, R., Bell, D., Cattley, R.C., Ferguson, S.S., Geter, D., Goetz, A., Goodman, J.I., Hester, S., Jacobs, A., Omiecinski, C.J., Schoeny, R., Xie, W., Lake, B.G., 2014. Mode of action and human relevance analysis for nuclear receptor-mediated liver toxicity: a case study with phenobarbital as a model constitutive androstane receptor (CAR) activator. Crit. Rev. Toxicol. 44, 64–82. https://doi.org/10.3109/10408444.2013.835786.
Ema, M., Fujii, S., Hirata-Koizumi, M., Matsumoto, M., 2008. Two-generation reproductive toxicity study of the flame retardant hexabromocyclododecane in rats. Reprod. Toxicol. 25, 335–351. https://doi.org/10.1016/j.reprotox.2007.12.004.
Farmahin, R., Williams, A., Kuo, B., Chepelev, N.L., Thomas, R.S., Barton-Maclaren, T., Curran, I.H., Nong, A., Wade, M., Yauk, C.L., 2016. Br/ > Recommended approaches in the application of toxicogenomics to derive points of departure for chemical risk assessment. Arch. Toxicol (in press).
Feng, M., Qu, R., Wang, C., Wang, L., Wang, Z., 2013. Comparative antioxidant status in freshwater fish Carassius auratus exposed to six current-use brominated flame retardants: a combined experimental and theoretical study. Aquat. Toxicol. 140–141, 314–323. https://doi.org/10.1016/j.aquatox.2013.07.001.
Fery, Y., Mueller, S.O., Schrenk, D., 2010. Development of stably transfected human and rat hepatoma cell lines for the species-specific assessment of xenobiotic response enhancer module (XREM)-dependent induction of drug metabolism. Toxicology 277, 11–19. https://doi.org/10.1016/j.tox.2010.08.008.
Fery, Y., Buschauer, I., Salzig, C., Lang, P., Schrenk, D., 2009. Technical pentabromodiphenyl ether and hexabromocyclododecane as activators of the pregnane-X-receptor (PXR). Toxicology 264, 45–51. https://doi.org/10.1016/j.tox.2009.07.009.
Firestone, M., Kavlock, R., Zenick, H., Kramer, M., US Environmental Protection Agency Working Group on the Future of Toxicity Testing, 2010. The U.S. Environmental Protection Agency strategic plan for evaluating the toxicity of chemicals. J. Toxicol. Environ. Health B Crit. Rev. 13, 139–162. https://doi.org/10.1080/10937404.2010.483178.
Formosa, A., Markert, E.K., Lena, A.M., Italiano, D., Finazzi-Agro, E., Levine, A.J., Bernardini, S., Garabadgiu, A.V., Melino, G., Candi, E., 2014. MicroRNAs, miR-154, miR-299-5p, miR-376a, miR-376c, miR-377, miR-381, miR-487b, miR-485-3p, miR-495 and miR-654-3p, mapped to the 14q32.31 locus, regulate proliferation, apoptosis, migration and invasion in metastatic prostate cancer cells. Oncogene 33, 5173–5182. https://doi.org/10.1038/onc.2013.451.
Fromme, H., Becher, G., Hilger, B., Volkel, W., 2016. Brominated flame retardants - exposure and risk assessment for the general population. Int. J. Hyg Environ. Health 219, 1–23. https://doi.org/10.1016/j.ijheh.2015.08.004.
Fromme, H., Hilger, B., Kopp, E., Miserok, M., Volkel, W., 2014. Polybrominated diphenyl ethers (PBDEs), hexabromocyclododecane (HBCD) and "novel" brominated flame retardants in house dust in Germany. Environ. Int. 64, 61–68. https://doi.org/10.1016/j.envint.2013.11.017.
Froy, O., 2010. Metabolism and circadian rhythms—implications for obesity. Endocr. Rev. 31, 1–24. https://doi.org/10.1210/er.2009-0014.
Gannon, A.M., Nunnikhoven, A., Liston, V., Rawn, D.F.K., Pantazopoulos, P., Fine, J.H., Caldwell, D., Bondy, G.S. and Curran, I.H.A., Submitted. Rat Strain Response Differences upon Exposure to Technical or Alpha Hexabromocyclododecane.
Germer, S., Piersma, A., van der Ven, L., Kamyschnikow, A., Fery, Y., Schmitz, H., Schrenk, D., 2006. Subacute effects of the brominated flame retardants hexabromocyclododecane and tetrabromobisphenol A on hepatic cytochrome P450 levels in rats. Toxicology 218, 229–236. https://doi.org/10.1016/j.tox.2005.10.019.
Gong, B., Wang, C., Su, Z., Hong, H., Thierry-Mieg, J., Thierry-Mieg, D., Shi, L., Auerbach, S.S., Tong, W., Xu, J., 2014. Transcriptomic profiling of rat liver samples in a comprehensive study design by RNA-Seq. Sci. Data 1, 140021. https://doi.org/10.1038/sdata.2014.21.
Guo, G.L., Staudinger, J., Ogura, K., Klaassen, C.D., 2002. Induction of rat organic anion transporting polypeptide 2 by pregnenolone-16alpha-carbonitrile is via interaction with pregnane X receptor. Mol. Pharmacol. 61, 832–839.
Gusenleitner, D., Auerbach, S.S., Melia, T., Gomez, H.F., Sherr, D.H., Monti, S., 2014. Genomic models of short-term exposure accurately predict long-term chemical carcinogenicity and identify putative mechanisms of action. PLoS One 9, e102579. https://doi.org/10.1371/journal.pone.0102579.
Hachisuka, A., Nakamura, R., Sato, Y., Nakamura, R., Shibutani, M., Teshima, R., 2010. Effects of perinatal exposure to the brominated flame-retardant hexabromocyclododecane (HBCD) on the developing immune system in rats. Kokuritsu Iyakuhin Shokuhin Eisei Kenkyusho. Hokoku 128, 58–64.
Hamers, T., Kamstra, J.H., Sonneveld, E., Murk, A.J., Kester, M.H., Andersson, P.L., Legler, J., Brouwer, A., 2006. In vitro profiling of the endocrine-disrupting potency of brominated flame retardants. Toxicol. Sci. 92, 157–173 kfj187.
Hartley, D.P., Dai, X., He, Y.D., Carlini, E.J., Wang, B., Huskey, S.E., Ulrich, R.G., Rushmore, T.H., Evers, R., Evans, D.C., 2004. Activators of the rat pregnane X receptor differentially modulate hepatic and intestinal gene expression. Mol. Pharmacol. 65, 1159–1171. https://doi.org/10.1124/mol.65.5.1159.
Hastie, T., Tibshirani, R., Narasimhan, B., Chu, G., 2014. pamr: Pam: prediction analysis for microarrays. R package version 1.55. http://CRAN.R-project.org/package=pamr.
Heindel, J.J., Newbold, R., Schug, T.T., 2015. Endocrine disruptors and obesity. Nat. Rev. Endocrinol. 11, 653–663.
Hernandez, J.P., Mota, L.C., Baldwin, W.S., 2009. Activation of CAR and PXR by dietary, environmental and occupational chemicals alters drug metabolism, intermediary metabolism, and cell proliferation. Curr. Pharmacogenomics Person Med. 7, 81–105. https://doi.org/10.2174/187569209788654005.
Hester, S., Eastmond, D.A., Bhat, V.S., 2015. Developing toxicogenomics as a research tool by applying benchmark dose-response modelling to inform chemical mode of action and tumorigenic potency. Int. J. Biotechnol. 14, 28. https://doi.org/10.1504/IJBT.2015.074796.
Hinkson, N.C., Whalen, M.M., 2010. Hexabromocyclododecane decreases tumor-cell-binding capacity and cell-surface protein expression of human natural killer cells. J. Appl. Toxicol. 30, 302–309. https://doi.org/10.1002/jat.1495.
Hinkson, N.C., Whalen, M.M., 2009. Hexabromocyclododecane decreases the lytic

function and ATP levels of human natural killer cells. J. Appl. Toxicol. 29, 656–661. https://doi.org/10.1002/jat.1453.
Hong, H., Shen, R., Liu, W., Li, D., Huang, L., Shi, D., 2015. Developmental toxicity of three hexabromocyclododecane diastereoisomers in embryos of the marine medaka Oryzias melastigma. Mar. Pollut. Bull. 101, 110–118. https://doi.org/10.1016/j.marpolbul.2015.11.009.
Hood, A., Klaassen, C.D., 2000. Differential effects of microsomal enzyme inducers on in vitro thyroxine (T(4)) and triiodothyronine (T(3)) glucuronidation. Toxicol. Sci. 55, 78–84.
Horvat, T., Landesmann, B., Lostia, A., Vinken, M., Munn, S., Whelan, M., 2017. Adverse outcome pathway development from protein alkylation to liver fibrosis. Arch. Toxicol. 91, 1523–1543. http://doi.org/10.1007/s00204-016-1814-8.
Hu, J., Liang, Y., Chen, M., Wang, X., 2009. Assessing the toxicity of TBBPA and HBCD by zebrafish embryo toxicity assay and biomarker analysis. Environ. Toxicol. 24, 334–342. https://doi.org/10.1002/tox.20436.
Ihunnah, C.A., Jiang, M., Xie, W., 2011. Nuclear receptor PXR, transcriptional circuits and metabolic relevance. Biochim. Biophys. Acta 1812, 956–963. https://doi.org/10.1016/j.bbadis.2011.01.014.
Jackson, A.F., Williams, A., Recio, L., Waters, M.D., Lambert, I.B., Yauk, C.L., 2014. Case study on the utility of hepatic global gene expression profiling in the risk assessment of the carcinogen furan. Toxicol. Appl. Pharmacol. 274, 63–77. https://doi.org/10.1016/j.taap.2013.10.019.
Kehrer, J.P., 2000. Cause-effect of oxidative stress and apoptosis. Teratology 62, 235–236. https://doi.org/10.1002/1096-9926(200010)62:4<235::AID-TERA11>3.0.CO;2-3.
Kiefer, F.W., Orasanu, G., Nallamshetty, S., Brown, J.D., Wang, H., Luger, P., Qi, N.R., Burant, C.F., Duester, G., Plutzky, J., 2012. Retinaldehyde dehydrogenase 1 coordinates hepatic gluconeogenesis and lipid metabolism. Endocrinology 153, 3089–3099. https://doi.org/10.1210/en.2011-2104.
Kodama, S., Negishi, M., 2011. Pregnane X receptor PXR activates the GADD45beta gene, eliciting the p38 MAPK signal and cell migration. J. Biol. Chem. 286, 3570–3578. https://doi.org/10.1074/jbc.M110.179812.
Kuo, B., Francina Webster, A., Thomas, R.S., Yauk, C.L., 2016. BDExpress Data Viewer - a visualization tool to analyze BMDExpress datasets. J. Appl. Toxicol. 36, 1048–1059.
Landesmann, B., 2016. Adverse Outcome Pathway on Protein Alkylation Leading to Liver Fibrosis. OECD Series on Adverse Outcome Pathways, No. 2. OECD Publishing, Paris, pp. 72. https://doi.org/10.1787/5jlsvwl6g7r5-en.
Langmead, B., Salzberg, S.L., 2012. Fast gapped-read alignment with Bowtie 2. Nat. Methods 9, 357–359. https://doi.org/10.1038/nmeth.1923.
Law, K., Halldorson, T., Danell, R., Stern, G., Gewurtz, S., Alaee, M., Marvin, C., Whittle, M., Tomy, G., 2006. Bioaccumulation and trophic transfer of some brominated flame retardants in a Lake Winnipeg (Canada) food web. Environ. Toxicol. Chem. 25, 2177–2186.
LeBlanc, G.A., Waxman, D.J., 1990. Mechanisms of cyclophosphamide action on hepatic P-450 expression. Cancer Res. 50, 5720–5726.
LeBlanc, G.A., Waxman, D.J., 1988. Feminization of rat hepatic P-450 expression by cisplatin. Evidence for perturbations in the hormonal regulation of steroid-metabolizing enzymes. J. Biol. Chem. 263, 15732–15739.
Li, G., Xie, Q., Shi, Y., Li, D., Zhang, M., Jiang, S., Zhou, H., Lu, H., Jin, Y., 2006. Inhibition of connective tissue growth factor by siRNA prevents liver fibrosis in rats. J. Gene Med. 8, 889–900. https://doi.org/10.1002/jgm.894.
Lignell, S., Aune, M., Glynn, A., Cantillana, T., 2015. Levels of PBDEs and HBCD in Blood Serum from first-time mothers in uppsala – temporal trends 1996-2014. available at: http://www.diva-portal.org/smash/get/diva2:806972/FULLTEXT01.pdf.
Lin, J., Huang, S., Wu, S., Ding, J., Zhao, Y., Liang, L., Tian, Q., Zha, R., Zhan, R., He, X., 2011. MicroRNA-423 promotes cell growth and regulates G(1)/S transition by targeting p21Cip1/Waf1 in hepatocellular carcinoma. Carcinogenesis 32, 1641–1647. https://doi.org/10.1093/carcin/bgr199.
Lipson, K.E., Wong, C., Teng, Y., Spong, S., 2012. CTGF is a central mediator of tissue remodeling and fibrosis and its inhibition can reverse the process of fibrosis. Fibrogenesis Tissue Repair 5, S24. https://doi.org/10.1186/1755-1536-5-S1-S24.
Liu, Z., Zanata, S.M., Kim, J., Peterson, M.A., Di Vizio, D., Chirieac, L.R., Pyne, S., Agostini, M., Freeman, M.R., Loda, M., 2013. The ubiquitin-specific protease USP2a prevents endocytosis-mediated EGFR degradation. Oncogene 32, 1660–1669. https://doi.org/10.1038/onc.2012.188.
Locker, J., Tian, J., Carver, R., Concas, D., Cossu, C., Ledda-Columbano, G.M., Columbano, A., 2003. A common set of immediate-early response genes in liver regeneration and hyperplasia. Hepatology 38, 314–325. https://doi.org/10.1053/jhep.2003.50299.
Love, M.I., Huber, W., Anders, S., 2014. Moderated estimation of fold change and dispersion for RNA-seq data with DESeq2. Genome Biol. 15. https://doi.org/10.1186/s13059-014-0550-8.
Maronpot, R.R., Yoshizawa, K., Nyska, A., Harada, T., Flake, G., Mueller, G., Singh, B., Ward, J.M., 2010. Hepatic enzyme induction: Histopathology. Toxicol. Pathol. 38, 776–795. https://doi.org/10.1177/0192623310373778.
Marvin, C.H., Tomy, G.T., Armitage, J.M., Arnot, J.A., McCarty, L., Covaci, A., Palace, V., 2011. Hexabromocyclododecane: current understanding of chemistry, environmental fate and toxicology and implications for global management. Environ. Sci. Technol. 45, 8613–8623. https://doi.org/10.1021/es201548c.
Masri, S., Sassone-Corsi, P., 2013. The circadian clock: a framework linking metabolism, epigenetics and neuronal function. Nat. Rev. Neurosci. 14, 69–75. https://doi.org/10.1038/nrn3393.
McCarthy, D.J., Chen, Y., Smyth, G.K., 2012. Differential expression analysis of multifactor RNA-Seq experiments with respect to biological variation. Nucleic Acids Res. 40, 4288–4297. https://doi.org/10.1093/nar/gks042.
Miao, F., Zhu, J., Chen, Y., Tang, N., Wang, X., Li, X., 2015. MicroRNA-183-5p promotes the proliferation, invasion and metastasis of human pancreatic adenocarcinoma cells. Oncol. Lett. https://doi.org/10.3892/ol.2015.3872.
Miao, H., Wei, B.R., Peehl, D.M., Li, Q., Alexandrou, T., Schelling, J.R., Rhim, J.S., Sedor, J.R., Burnett, E., Wang, B., 2001. Activation of EphA receptor tyrosine kinase inhibits the Ras/MAPK pathway. Nat. Cell Biol. 3, 527–530. https://doi.org/10.1038/35074604.
Miller, I., Serchi, T., Cambier, S., Diepenbroek, C., Renaut, J., Van der Berg, J.H., Kwadijk, C., Gutleb, A.C., Rijntjes, E., Murk, A.J., 2016a. Hexabromocyclododecane (HBCD) induced changes in the liver proteome of eu- and hypothyroid female rats. Toxicol. Lett. 245, 40–51. https://doi.org/10.1016/j.toxlet.2016.01.002.
Miller, I., Diepenbroek, C., Rijntjes, E., Renaut, J., Teerds, K.J., Kwadijk, C., Cambier, S., Murk, A.J., Gutleb, A.C., Serchi, T., 2016b. Gender specific differences in the liver proteome of rats exposed to short term and low-concentration hexabromocyclododecane (HBCD). Toxicol. Res. 5 (5), 1273–1283. https://doi.org/10.1039/c6tx00166a.
Moffat, I., Chepelev, N.L., Labib, S., Bourdon-Lacombe, J., Kuo, B., Buick, J.K., Lemieux, F., Williams, A., Halappanavar, S., Malik, A.I., Luijten, M., Aubrecht, J., Hyduke, D.R., Fornace Jr., A.J., Swartz, C.D., Recio, L., Yauk, C.L., 2015. Comparison of toxicogenomics and traditional approaches to inform mode of action and points of departure in human health risk assessment of benzo[a]pyrene in drinking water. Crit. Rev. Toxicol. 45, 1–43. https://doi.org/10.3109/10408444.2014.973934.
Musiek, E.S., 2015. Circadian clock disruption in neurodegenerative diseases: cause and effect? Front. Pharmacol. 6. https://doi.org/10.3389/fphar.2015.00029.
Nakamura, S., Nagata, Y., Tan, L., Takemura, T., Shibata, K., Fujie, M., Fujisawa, S., Tanaka, Y., Toda, M., Makita, R., Tsunekawa, K., Yamada, M., Yamaoka, M., Yamashita, J., Ohnishi, K., Yamashita, M., 2011. Transcriptional repression of Cdc25B by IER5 inhibits the proliferation of leukemic progenitor cells through NF-YB and p300 in acute myeloid leukemia. PLoS One 6, e28011. https://doi.org/10.1371/journal.pone.0028011.
Nakano, H., Shizu, R., Benoki, S., Numakura, Y., Kodama, S., Miyata, M., Yamazoe, Y., Yoshinari, K., 2013. Xenobiotic-induced hepatocyte proliferation associated with constitutive active/androstane receptor (CAR) or peroxisome proliferator-activated receptor a (PPARa) is enhanced by pregnane X receptor (PXR) activation in mice. PLoS One 8, e61802. https://doi.org/10.1371/journal.pone.0061802.
Nepal, S., Shrestha, A., Park, P.H., 2015. Ubiquitin specific protease 2 acts as a key modulator for the regulation of cell cycle by adiponectin and leptin in cancer cells. Mol. Cell. Endocrinol. 412, 44–55. https://doi.org/10.1016/j.mce.2015.05.029.
Novak, K., 2005. Signalling: turning off the tap. Nat. Rev. Canc. 5, 754. https://doi.org/10.1038/nrc1722.
[NTP] National Toxicology Program, 2018. Research Report on National Toxicology Program Approach to Genomic Dose-response Modeling. Research Report 5. Public Health Service, U.S. Department of Health and Human Services ISSN: 2473-4756. https://ntp.niehs.nih.gov/ntp/results/pubs/rr/reports/rr05_508.pdf.
Okayama, T., Kikuchi, S., Ochiai, T., Ikoma, H., Kubota, T., Ichikawa, D., Fujiwara, H., Okamoto, K., Sakakura, C., Sonoyama, T., Kokuba, Y., Doi, Y., Tsukita, S., Bissell, D.M., Otsuji, E., 2008. Attenuated response to liver injury in moesin-deficient mice: impaired stellate cell migration and decreased fibrosis. Biochim. Biophys. Acta 1782, 542–548. https://doi.org/10.1016/j.bbadis.2008.06.006.
Palace, V., Park, B., Pleskach, K., Gemmill, B., Tomy, G., 2010. Altered thyroxine metabolism in rainbow trout (Oncorhynchus mykiss) exposed to hexabromocyclododecane (HBCD). Chemosphere 80, 165–169. https://doi.org/10.1016/j.chemosphere.2010.03.016.
Palace, V.P., Pleskach, K., Halldorson, T., Danell, R., Wautier, K., Evans, B., Alaee, M., Marvin, C., Tomy, G.T., 2008. Biotransformation enzymes and thyroid Axis disruption in Juvenile rainbow trout (Oncorhynchus mykiss) exposed to hexabromocyclododecane diastereoisomers. Environ. Sci. Technol. 42, 1967–1972. https://doi.org/10.1021/es702565h.
Partch, C.L., Green, C.B., Takahashi, J.S., 2014. Molecular architecture of the mammalian circadian clock. Trends Cell Biol. 24, 90–99. https://doi.org/10.1016/j.tcb.2013.07.002.
Peng, Y., Rideout, D., Rakita, S., Sajan, M., Farese, R., You, M., Murr, M.M., 2009. Downregulation of adiponectin/AdipoR2 is associated with steatohepatitis in obese mice. J. Gastrointest. Surg. 13, 2043–2049. https://doi.org/10.1007/s11605-009-1032-2.
Petrosino, J.M., Disilvestro, D., Ziouzenkova, O., 2014. Aldehyde dehydrogenase 1A1: friend or foe to female metabolism? Nutrients 6, 950–973. https://doi.org/10.3390/nu6030950.
Phillips, J., Svoboda, D., Tandon, A., Patel, S., Sedykh, A., Mav, D., Kuo, B., Yauk, C., Yang, L., Thomas, R., Gift, J., Davis, A., Olysyzk, L., Parham, P., Saddler, T., Shah, R., Auerbach, S., 2018 Oct 17. BMDExpress 2: enhanced transcriptomic dose-response analysis workflow. Bioinformatics. https://doi.org/10.1093/bioinformatics/bty878. [Epub ahead of print], PMID: 30329029.
Pratt, R.L., Kinch, M.S., 2002. Activation of the EphA2 tyrosine kinase stimulates the MAP/ERK kinase signaling cascade. Oncogene 21, 7690–7699. https://doi.org/10.1038/sj.onc.1205758.
Qin, X., Xie, X., Fan, Y., Tian, J., Guan, Y., Wang, X., Zhu, Y., Wang, N., 2008. Peroxisome proliferator-activated receptor-delta induces insulin-induced gene-1 and suppresses hepatic lipogenesis in obese diabetic mice. Hepatology 48, 432–441. https://doi.org/10.1002/hep.22334.
R Core Team, 2015. R: a Language and Environment for Statistical Computing. R Foundation for Statistical Computing, Vienna, Austria. http://www.R-project.org/.
Reeves, P.G., 1997. Components of the AIN-93 diets as improvements in the AIN-76A diet. J. Nutr. 127, 838S–841S.
Reichert, A.S., Reglinski, K., Keil, M., Altendorf, S., Waithe, D., Eggeling, C., Schliebs, W., Erdmann, R., 2015. Peroxisomal import reduces the proapoptotic activity of deubiquitinating enzyme USP2. PLoS One 10, e0140685. https://doi.org/10.1371/journal.

pone.0140685.
Reichert, B., Yasmeen, R., Jeyakumar, S.M., Yang, F., Thomou, T., Alder, H., Duester, G., Maiseyeu, A., Mihai, G., Harrison, E.H., Rajagopalan, S., Kirkland, J.L., Ziouzenkova, O., 2011. Concerted action of aldehyde dehydrogenases influences depot-specific fat formation. Mol. Endocrinol. 25, 799–809. https://doi.org/10.1210/me.2010-0465.
Reistad, T., Fonnum, F., Mariussen, E., 2006. Neurotoxicity of the pentabrominated diphenyl ether mixture, DE-71, and hexabromocyclododecane (HBCD) in rat cerebellar granule cells in vitro. Arch. Toxicol. 80, 785–796. https://doi.org/10.1007/s00204-006-0099-8.
Richardson, V., DeVito, M.J., 2008. In Vitro Metabolism of Thyroid Hormone by Recombinant Human UDP-glucuronosyltransferase and Sulfotransferase. March 16 - 20. Presented at Society of Toxicology Annual Meeting, Seattle, WA.
Robinson, M.D., Oshlack, A., 2010. A scaling normalization method for differential expression analysis of RNA-seq data. Genome Biol. 11https://doi.org/10.1186/gb-2010-11-3-r25. R25-2010-11-3-r25. Epub 2010 Mar 2.
Robinson, M.W., Harmon, C., O'Farrelly, C., 2016. Liver immunology and its role in inflammation and homeostasis. Cell. Mol. Immunol. 13, 267–276. https://doi.org/10.1038/cmi.2016.3.
Roze, E., Meijer, L., Bakker, A., Van Braeckel, K.N., Sauer, P.J., Bos, A.F., 2009. Prenatal exposure to organohalogens, including brominated flame retardants, influences motor, cognitive, and behavioral performance at school age. Environ. Health Perspect. 117, 1953–1958. https://doi.org/10.1289/ehp.0901015.
Saegusa, Y., Fujimoto, H., Woo, G.H., Inoue, K., Takahashi, M., Mitsumori, K., Hirose, M., Nishikawa, A., Shibutani, M., 2009. Developmental toxicity of brominated flame retardants, tetrabromobisphenol A and 1,2,5,6,9,10-hexabromocyclododecane, in rat offspring after maternal exposure from mid-gestation through lactation. Reprod. Toxicol. 28, 456–467. https://doi.org/10.1016/j.reprotox.2009.06.011.
Sahar, S., Sassone-Corsi, P., 2009. Metabolism and cancer: the circadian clock connection. Nat. Rev. Canc. 9, 886–896. https://doi.org/10.1038/nrc2747.
Saito, K., Kaneko, H., Sato, K., Yoshitake, A., Yamada, H., 1991. Hepatic UDP-glucuronyltransferase(s) activity toward thyroid hormones in rats: induction and effects on serum thyroid hormone levels following treatment with various enzyme inducers. Toxicol. Appl. Pharmacol. 111, 99–106.
Sanjurjo, L., Aran, G., Roher, N., Valledor, A.F., Sarrias, M.R., 2015. AIM/CD5L: a key protein in the control of immune homeostasis and inflammatory disease. J. Leukoc. Biol. 98, 173–184. https://doi.org/10.1189/jlb.3RU0215-074R.
Sato, M., Bremner, I., 1993. Oxygen free radicals and metallothionein. Free Radic. Biol. Med. 14, 325–337.
Savvidis, C., Koutsilieris, M., 2012. Circadian rhythm disruption in cancer biology. Mol. Med. 18, 1249–1260. https://doi.org/10.2119/molmed.2012.00077.
Scheiermann, C., Kunisaki, Y., Frenette, P.S., 2013. Circadian control of the immune system. Nat. Rev. Immunol. 13, 190–198. https://doi.org/10.1038/nri3386.
Shin, J.U., Lee, W.J., Tran, T.N., Jung, I., Lee, J.H., 2015. Hsp70 knockdown by siRNA decreased collagen production in keloid fibroblasts. Yonsei Med. J. 56, 1619–1626. https://doi.org/10.3349/ymj.2015.56.6.1619.
Tan, X., Zhao, T., Wang, Z., Wang, J., Wang, Y., Liu, Z., Liu, X., 2018. acrylamide defects the expression pattern of the circadian clock and mitochondrial dynamics in C57BL/6J mice liver and HepG2 cells. J. Agric. Food Chem. https://doi.org/10.1021/acs.jafc.8b02473.
Tarazona, S., Furio-Tari, P., Turra, D., Pietro, A.D., Nueda, M.J., Ferrer, A., Conesa, A., 2015. Data quality aware analysis of differential expression in RNA-seq with NOISeq R/Bioc package. Nucleic Acids Res. 43, e140. https://doi.org/10.1093/nar/gkv711.
Thierry-Mieg, D., Thierry-Mieg, J., 2006. AceView: a comprehensive cDNA-supported gene and transcripts annotation. S12.1-14. Genome Biol. 7 (Suppl. 1) gb-2006-7-s1-s12.
Thomas, R.S., Philbert, M.A., Auerbach, S.S., Wetmore, B.A., Devito, M.J., Cote, I., Rowlands, J.C., Whelan, M.P., Hays, S.M., Andersen, M.E., Meek, M.E., Reiter, L.W., Lambert, J.C., Clewell 3rd, H.J., Stephens, M.L., Zhao, Q.J., Wesselkamper, S.C., Flowers, L., Carney, E.W., Pastoor, T.P., Petersen, D.D., Yauk, C.L., Nong, A., 2013a. Incorporating new technologies into toxicity testing and risk assessment: moving from 21st century vision to a data-driven framework. Toxicol. Sci. 136, 4–18. https://doi.org/10.1093/toxsci/kft178.
Thomas, R.S., Wesselkamper, S.C., Wang, N.C.Y., Zhao, Q.J., Petersen, D.D., Lambert, J.C., Cote, I., Yang, L., Healy, E., Black, M.B., Clewell, H.J., Allen, B.C., Andersen, M.E., 2013b. Temporal concordance between apical and transcriptional points of departure for chemical risk assessment. Toxicol. Sci. 134, 180–194. https://doi.org/10.1093/toxsci/kft094.
Thomas, R.S., Clewell 3rd, H.J., Allen, B.C., Wesselkamper, S.C., Wang, N.C., Lambert, J.C., Hess-Wilson, J.K., Zhao, Q.J., Andersen, M.E., 2011. Application of transcriptional benchmark dose values in quantitative cancer and noncancer risk assessment. Toxicol. Sci. 120, 194–205. https://doi.org/10.1093/toxsci/kfq355.
Thomas, R.S., Allen, B.C., Nong, A., Yang, L., Bermudez, E., Clewell, H.J., Andersen, M.E., 2007. A method to integrate benchmark dose estimates with genomic data to assess the functional effects of chemical exposure. Toxicol. Sci. 98, 240–248. https://doi.org/10.1093/toxsci/kfm092.
Tian, J., Huang, H., Hoffman, B., Liebermann, D.A., Ledda-Columbano, G.M., Columbano, A., Locker, J., 2011. Gadd45ß is an inducible coactivator of transcription that facilitates rapid liver growth in mice. J. Clin. Invest. 121, 4491–4502. https://doi.org/10.1172/JCI38760.
Tibshirani, R., Hastie, T., Narasimhan, B., Chu, G., 2002. Diagnosis of multiple cancer types by shrunken centroids of gene expression. Proc. Natl. Acad. Sci. U. S. A. 99, 6567–6572. https://doi.org/10.1073/pnas.082099299.
Tomita, K., Oike, Y., Teratani, T., Taguchi, T., Noguchi, M., Suzuki, T., Mizutani, A., Yokoyama, H., Irie, R., Sumimoto, H., Takayanagi, A., Miyashita, K., Akao, M., Tabata, M., Tamiya, G., Ohkura, T., Hibi, T., 2008. Hepatic AdipoR2 signaling plays a protective role against progression of nonalcoholic steatohepatitis in mice. Hepatology 48, 458–473. https://doi.org/10.1002/hep.22365.
Trachootham, D., Lu, W., Ogasawara, M.A., Nilsa, R.D., Huang, P., 2008. Redox regulation of cell survival. Antioxid. Redox Signal. 10, 1343–1374. https://doi.org/10.1089/ars.2007.1957.
Tsang, A.H., Barclay, J.L., Oster, H., 2013. Interactions between endocrine and circadian systems. J. Mol. Endocrinol. 52, R1–R16. https://doi.org/10.1530/JME-13-0118.
UNEP, 2013a. Report of the conference of the parties to the Stockholm convention on persistent organic Pollutants on the work of its sixth meeting- document POPS/COP.6/33. available at: http://chm.pops.int/TheConvention/ConferenceoftheParties/ReportsandDecisions.
UNEP, 2013b. Decision SC-6/13: listing of hexabromocyclododecane. available at: http://chm.pops.int/Portals/0/download.aspx?d=UNEP-POPS-COP.6-SC-6-13.English.pdf.
van der Ven, L.T., van de Kuil, T., Leonards, P.E., Slob, W., Lilienthal, H., Litens, S., Herlin, M., Hakansson, H., Canton, R.F., van den Berg, M., Visser, T.J., van Loveren, H., Vos, J.G., Piersma, A.H., 2009. Endocrine effects of hexabromocyclododecane (HBCD) in a one-generation reproduction study in Wistar rats. Toxicol. Lett. 185, 51–62. https://doi.org/10.1016/j.toxlet.2008.12.003.
van der Ven, L.T., Verhoef, A., van de Kuil, T., Slob, W., Leonards, P.E., Visser, T.J., Hamers, T., Herlin, M., Hakansson, H., Olausson, H., Piersma, A.H., Vos, J.G., 2006. A 28-day oral dose toxicity study enhanced to detect endocrine effects of hexabromocyclododecane in Wistar rats. Toxicol. Sci. 94, 281–292 kfl113.
Vansell, N.R., Klaassen, C.D., 2002. Effect of microsomal enzyme inducers on the biliary excretion of triiodothyronine (T(3)) and its metabolites. Toxicol. Sci. 65, 184–191.
Vinken, M., 2013. The adverse outcome pathway concept: a pragmatic tool in toxicology. Toxicology 312, 158–165. https://doi.org/10.1016/j.tox.2013.08.011.
Visser, T.J., Kaptein, E., Gijzel, A.L., de Herder, W.W., Ebner, T., Burchell, B., 1993. Glucuronidation of thyroid hormone by human bilirubin and phenol UDP-glucuronyltransferase isoenzymes. FEBS Lett. 324, 358–360 0014-5793(93)80151-J.
Wang, C., Chen, J., Cao, W., Sun, L., Sun, H., Liu, Y., 2016a. Aurora-B and HDAC synergistically regulate survival and proliferation of lymphoma cell via AKT, mTOR and Notch pathways. Eur. J. Pharmacol. 779, 1–7. https://doi.org/10.1016/j.ejphar.2015.11.049.
Wang, F., Zhang, H., Geng, N., Zhang, B., Ren, X., Chen, J., 2016b. New insights into the cytotoxic mechanism of hexabromocyclododecane from a metabolomic approach. Environ. Sci. Technol. 50, 3145–3153. https://doi.org/10.1021/acs.est.5b03678.
Wang, H., Cao, F., Li, X., Miao, H., E, J., Xing, J., Fu, C.G., 2015. miR-320b suppresses cell proliferation by targeting c-Myc in human colorectal cancer cells. BMC Canc. 15https://doi.org/10.1186/s12885-015-1728-5. 748-015-1728-5.
Wania, F., Dugani, C.B., 2003. Assessing the long-range transport potential of polybrominated diphenyl ethers: a comparison of four multimedia models. Environ. Toxicol. Chem. 22, 1252–1261.
Webster, A.F., Chepelev, N., Gagné, R., Kuo, B., Recio, L., Williams, A., Yauk, C.L., 2015. Impact of genomics platform and statistical filtering on transcriptional benchmark doses (BMD) and multiple approaches for selection of chemical point of departure (PoD). PLoS One 10 (8), e0136764. https://doi.org/10.1371/journal.pone.0136764.eCollection 2015.
Wei, P., Zhang, J., Egan-Hafley, M., Liang, S., Moore, D.D., 2000. The nuclear receptor CAR mediates specific xenobiotic induction of drug metabolism. Nature 407, 920–923. https://doi.org/10.1038/35038112.
Wen, Q., Zhang, D., Wang, T., Wang, T., Zhao, M., Xie, Q., Fu, Y., Ma, Q., 2016. MiR-23a promotes cell proliferation and invasion in papillary thyroid carcinoma by targeting PTEN < br/ > Int. J. Clin. Exp. Pathol. 9, 2366–2373.
Willett, C., Caverly Rae, J., Goyak, K.O., Landesmann, B., Minsavage, G., Westmoreland, C., 2014. Pathway-based toxicity: history, current approaches and liver fibrosis and steatosis as prototypes. ALTEX 31, 407–421. https://doi.org/10.14573/altex.1401283.
Williams, D.A., 1971. A test for differences between treatment means when several dose levels are compared with a zero dose control. Biometrics 27 (1), 103–107.
Xiao, Y., Yan, W., Lu, L., Wang, Y., Lu, W., Cao, Y., Cai, W., 2015. p38/p53/miR-200a-3p feedback loop promotes oxidative stress-mediated liver cell death. Cell Cycle 14, 1548–1558. https://doi.org/10.1080/15384101.2015.1026491.
Xie, Q., Yan, Y., Huang, Z., Zhong, X., Huang, L., 2014. MicroRNA-221 targeting PI3-K/Akt signaling axis induces cell proliferation and BCNU resistance in human glioblastoma. Neuropathology 34, 455–464. https://doi.org/10.1111/neup.12129.
Yamada-Okabe, T., Sakai, H., Kashima, Y., Yamada-Okabe, H., 2005. Modulation at a cellular level of the thyroid hormone receptor-mediated gene expression by 1,2,5,6,9,10-hexabromocyclododecane (HBCD), 4,4'-diiodobiphenyl (DIB), and nitrofen (NIP). Toxicol. Lett. 155, 127–133. https://doi.org/10.1016/j.toxlet.2004.09.005.
Yamamoto, Y., Moore, R., Flavell, R.A., Lu, B., Negishi, M., 2010. Nuclear receptor CAR represses TNFalpha-induced cell death by interacting with the anti-apoptotic GADD45B. PLoS One 5, e10121. https://doi.org/10.1371/journal.pone.0010121.
Yamanaka, H., Nakajima, M., Katoh, M., Yokoi, T., 2007. Glucuronidation of thyroxine in human liver, Jejunum, and kidney microsomes. Drug Metab. Dispos. 35, 1642–1648. https://doi.org/10.1124/dmd.107.016097.
Yan, W., Chen, X., 2006. GPX2, a direct target of p63, inhibits oxidative stress-induced apoptosis in a p53-dependent manner. J. Biol. Chem. 281, 7856–7862 doi: M512655200 [pii].
Yanagisawa, R., Koike, E., Win-Shwe, T.T., Yamamoto, M., Takano, H., 2014. Impaired lipid and glucose homeostasis in hexabromocyclododecane-exposed mice fed a high-fat diet. Environ. Health Perspect. 122, 277–283. https://doi.org/10.1289/ehp.1307421.
Yang, F., Zhang, X., Maiseyeu, A., Mihai, G., Yasmeen, R., DiSilvestro, D., Maurya, S.K., Periasamy, M., Bergdall, K.V., Duester, G., Sen, C.K., Roy, S., Lee, L.J., Rajagopalan, S., Ziouzenkova, O., 2012. The prolonged survival of fibroblasts with forced lipid

catabolism in visceral fat following encapsulation in alginate-poly-L-lysine. Biomaterials 33, 5638–5649. https://doi.org/10.1016/j.biomaterials.2012.04.035.
Yang, L., Allen, B.C., Thomas, R.S., 2007. BMDExpress: a software tool for the benchmark dose analyses of genomic data. BMC Genomics 8, 387. https://doi.org/10.1186/1471-2164-8-387.
Yang, Y., Duguay, D., Fahrenkrug, J., Cermakian, N., Wing, S.S., 2014. USP2 regulates the intracellular localization of PER1 and circadian gene expression. J. Biol. Rhythm. 29, 243–256. https://doi.org/10.1177/0748730414544741.
Yang, Y., Sharma, R., Zimniak, P., Awasthi, Y.C., 2002. Role of a class glutathione S-transferases as antioxidant enzymes in rodent tissues. Toxicol. Appl. Pharmacol. 182, 105–115. https://doi.org/10.1006/taap.2002.9450.
Ye, H., Yu, X., Xia, J., Tang, X., Tang, L., Chen, F., 2016. MiR-486-3p targeting ECM1 represses cell proliferation and metastasis in cervical cancer. Biomed. Pharmacother. 80, 109–114. https://doi.org/10.1016/j.biopha.2016.02.019.
Ye, R., Selby, C.P., Chiou, Y.Y., Ozkan-Dagliyan, I., Gaddameedhi, S., Sancar, A., 2014. Dual modes of CLOCK:BMAL1 inhibition mediated by Cryptochrome and Period proteins in the mammalian circadian clock. Genes Dev. 28, 1989–1998. https://doi.org/10.1101/gad.249417.114.
Zeller, H., Kirsch, P., 1970. Hexabromocyclododecane: 90-day Feeding Trials with Rats. Pharmakologisches Institute, BASF Institute for Industrial Hygiene and Pharmacology, Federal Republic of Germany EPA/OTS Doc. #86–900000380.
Zeller, H., Kirsch, P., 1969. Hexabromocyclododecane: 28-day Feeding Trials with Rats. BASF Institute for Industrial Hygiene and Pharmacology, Federal Republic of Germany EPA/OTS Doc. #86–900000376.
ZHANG, W., LIU, H.T., 2002. MAPK signal pathways in the regulation of cell proliferation in mammalian cells. Cell Res. 12, 9–18. https://doi.org/10.1038/sj.cr.7290105.
Zhang, X., Yang, F., Xu, C., Liu, W., Wen, S., Xu, Y., 2008a. Cytotoxicity evaluation of three pairs of hexabromocyclododecane (HBCD) enantiomers on Hep G2 cell. Toxicol. In. Vitro. 22, 1520–1527. https://doi.org/10.1016/j.tiv.2008.05.006.
Zhang, X., Yang, F., Zhang, X., Xu, Y., Liao, T., Song, S., Wang, J., 2008b. Induction of hepatic enzymes and oxidative stress in Chinese rare minnow (Gobiocypris rarus) exposed to waterborne hexabromocyclododecane (HBCDD). Aquat. Toxicol. 86, 4–11 S0166-445X(07)00270-6.
Zhang, Y., Zheng, D., Xiong, Y., Xue, C., Chen, G., Yan, B., Ye, Q., 2014. miR-202 suppresses cell proliferation in human hepatocellular carcinoma by downregulating LRP6 post-transcriptionally. FEBS Lett. 588, 1913–1920. https://doi.org/10.1016/j.febslet.2014.03.030.
Zhang, Y., Cheng, X., Aleksunes, L., Klaassen, C.D., 2012. Transcription factor-mediated regulation of carboxylesterase enzymes in livers of mice. Drug Metab. Dispos. 40, 1191–1197. https://doi.org/10.1124/dmd.111.043877.
Zhu, K., Ding, H., Wang, W., Liao, Z., Fu, Z., Hong, Y., Zhou, Y., Zhang, C.Y., Chen, X., 2016. Tumor-suppressive miR-218-5p inhibits cancer cell proliferation and migration via EGFR in non-small cell lung cancer. Oncotarget 7, 28075–28085. https://doi.org/10.18632/oncotarget.8576.